

Portland State University

PDXScholar

Dissertations and Theses

Dissertations and Theses

6-21-1985

Copper Electrodeposition in a Magnetic Field

Hiroshi Takeo

Portland State University

Follow this and additional works at: https://pdxscholar.library.pdx.edu/open_access_etds



Part of the [Biological and Chemical Physics Commons](#)

Let us know how access to this document benefits you.

Recommended Citation

Takeo, Hiroshi, "Copper Electrodeposition in a Magnetic Field" (1985). *Dissertations and Theses*. Paper 3550.

<https://doi.org/10.15760/etd.5438>

This Thesis is brought to you for free and open access. It has been accepted for inclusion in Dissertations and Theses by an authorized administrator of PDXScholar. Please contact us if we can make this document more accessible: pdxscholar@pdx.edu.

AN ABSTRACT OF THE THESIS OF Hiroshi Takeo for the Master of Science in Physics presented June 21, 1985.

Title: Copper Electrodeposition in a Magnetic Field

APPROVED BY MEMBERS OF THE THESIS COMMITTEE:

[REDACTED]
John Dash, Chairperson

[REDACTED]
Carl G. Bachhuber

[REDACTED]
Donald G. Howard

[REDACTED]
Nan-Teh Hsu

The effect of a magnetic field on copper electrodeposition was investigated. Copper was electrodeposited onto square copper cathodes 1 sq cm in area from an aqueous solution (0.5 M CuSO_4 , $0.5 \text{ M H}_2\text{SO}_4$). A glass cell was placed between the pole pieces of an electromagnet, and the magnetic fields applied were in the range from 0 to 12.5 kG. The current density was in the range from 80 mA/sq cm to 880 mA/sq cm. In each of the experiments, cell current, cell voltage, and cell

temperature were monitored with a microcomputer. The weight change, deposit surface and cross section morphology, and hardness were also found. Anodes used in the experiments were studied to see the effect of various conditions on the surface finish. Copper was also electrodeposited onto copper grids in order to study how the uniformity of the deposit is affected by an applied magnetic field.

The results show that the deposit uniformity could be altered so that the deposit preserved the original shape of the holes on the copper grids. Also the smoothness of the deposit on the square cathodes could be altered. The limiting current can be increased by applying a suitable magnetic field, and the concentration overpotential is reduced.

Reduction of the concentration overpotential and increase of the limiting current arises largely due to the stirring effect which occurs because of the Lorentz force on the ions in solution. As with mechanical stirring, the forced convection aids the transport of ions to the cathode, and also reduces the thickness of the diffusion layer. Reduction of the diffusion layer thickness increases the concentration gradient near the electrode thereby enhancing the diffusion current.

The increase in deposit uniformity is attributed to improved electrolyte circulation, and also the

magnetoresistance caused by the deflection of the ions through the Lorentz force and an ionic Hall-effect. The magneto-produced stirring effect is greatest where the electric field is the largest. This means that the effect of the magnetoresistance may also be greatest in regions where the deposit would otherwise be thickest in the absence of an applied magnetic field, and growth of the deposit in such regions is hindered.

COPPER ELECTRODEPOSITION
IN A MAGNETIC FIELD

by
HIROSHI TAKEO

A thesis submitted in partial fulfillment of the
requirements for the degree of

MASTER OF SCIENCE
in
PHYSICS

Portland State University

1985

TO THE OFFICE OF GRADUATE STUDIES AND RESEARCH:

The members of the Committee approve the thesis of
Hiroshi Takeo presented June 21, 1985.

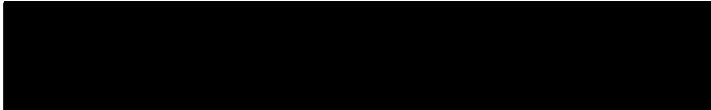

John Dash, Chairperson


Carl G. Bachhuber


Donald G. Howard


Nan-Teh Hsu

APPROVED:


R. W. Sommerfeldt, Head, Department of Physics


Jim F. Heath, Dean of Graduate Studies and Research

ACKNOWLEDGEMENTS

I would like to express my gratitude to Dr. John Dash for his patience, guidance and insight throughout the course of this research.

I am glad to have met Dr. Arash Kasaaian with whom I spent many hours in discussion and lunch-eating.

The data collection was accomplished smoothly because of the work of Mr. Craig Cousins prior to my inheriting the AIM 65 computer system.

I will not forget the much welcomed inspiration and suggestions given by my sibling graduate students.

The help of Ms. (Sobhana) Mal, Ms. Ching Tam, Ms. Kathleen Martin, and Mr. Brian Litzenberger was greatly appreciated. I am grateful to Mr. Garo Arkelian, Mr. Rudi Zupan, Mr. Brian McLaughlin, and Mr. Don Boileau who were always willing to lend their expertise. I also wish to thank Ms. Camille Hansen for her help with the word processor.

It suffices to say that nothing would be possible without the sacrifices and support of my parents. Finally, this thesis would have been impossible without the strength and understanding of my wife Alison, who gave me the freedom to pursue this work during an awkward period in our lives.

TABLE OF CONTENTS

	PAGE
ACKNOWLEDGEMENTS	iii
LIST OF TABLES	vi
LIST OF FIGURES	vii
CHAPTER	
I INTRODUCTION	1
Fundamentals	1
The interphase region	3
Contributors to the cell potential and their effects	5
Additional influences on electrodeposition	10
Stirring	10
Diffusion layer and diffusion	11
Magnetoresistance	13
II THE EXPERIMENT AND ANALYSIS	
Experimental apparatus and procedures	14
Analysis	23
Hardness testing	23
Microscopy	25
III EFFECT OF AN APPLIED MAGNETIC FIELD ON LIMITING CURRENT AND DEPOSITION ENERGY	26
Definition of quantities	26
Deposition energy	26
Method one	27

		v
	Method two	27
	Efficiency	28
	Experimental results and discussion . .	30
	Effect of varying the magnetic field on the efficiency	31
	DE versus applied B field	35
IV	EFFECT ON THE UNIFORMITY OF THE DEPOSIT . .	45
	Factors affecting the uniformity	45
	Current distribution	45
	Surface structure effects	46
	Addition agents	48
	Solution resistivity and throwing power	49
	Results and discussion	50
	Deposition onto TEM grids	54
	Findings of other workers	61
V	SURFACE MORPHOLOGY OF THE ANODES	64
	Discussion	70
VI	MECHANICAL PROPERTIES: HARDNESS	75
	Results	75
	Discussion	85
VII	CONCLUSION	92
	REFERENCES	94

LIST OF TABLES

TABLE		PAGE
I	Lower current density experimental data with smaller diameter cell	32
II	Low current density experimental data with larger diameter cell	33
III	High current density experimental data with with larger diameter cell	34
IV	Hardness of deposits and substrate for smaller diameter cell	78
V	Hardness of deposits and substrate for 80 mA/sq cm with larger diameter cell . .	81
VI	Hardness of deposits and substrate for higher current density with larger diameter cell	86

LIST OF FIGURES

FIGURE		PAGE
1.	Schematic diagram of typical copper deposition cell	2
2.	Schematic representation of polarization types	4
3.	How concentration polarization appears	9
4.	Diagram of cell	15
5.	Diagram of experimental set-up	19
6.	Cross sectioning of deposit for hardness testing	24
7.	Effect of a magnetic field on energy of deposition	37
8.	Typical voltage versus time graphs	39
9.	Current density-cell voltage drop relationship for a flow cell	42
10.	SEM micrographs of deposits at low magnetic fields	51
11.	SEM micrographs of deposits with doubled current density	52
12.	SEM micrographs of deposits for higher current densities, 190 and 360 mA/sq cm	55
13.	SEM micrograph of deposit 880 mA/sq cm	56

14.	Full view of copper grids for through-hole plating	57
15.	Magnified view of copper grids for through-hole plating	59
16.	Effect of applied magnetic field on current distribution	63
17.	SEM micrographs of anodes at low magnetic fields and low current density	66
18.	SEM micrographs of anodes showing effect of doubling the current density	67
19.	SEM micrographs of copper anodes at higher current density, 190 and 360 mA/sq cm	68
20.	SEM micrographs of copper anodes at 560 and 880 mA/sq cm	69
21.	Typical anode current density versus cell voltage characteristics	71
22.	Knoop hardness cross sections	77
23.	Hardness versus magnetic field, perpendicular orientation for experiments performed in the smaller diameter cell	79
24.	Hardness versus magnetic field, parallel orientation for experiments performed in the smaller diameter cell	80

25.	Hardness versus magnetic field, perpendicular orientation for experiments performed in the larger diameter cell	83
26.	Hardness versus magnetic field, parallel orientation for experiments performed in the larger diameter cell	84
27.	Hardness versus current density, perpendicular and parallel orientations	87
28.	Examples of deposits obtainable	91

CHAPTER I

INTRODUCTION

The task of studying the effect of an applied magnetic field on the copper electrodeposition process was chosen with the hopes of obtaining freshly useful and interesting results. Also, there was a desire to further our understanding of a system which we had observed in the past (1, 2, 3). Increasing the rate of copper deposition from the electrolyte, decreasing the energy required for producing deposits, observing effects on the uniformity of the deposit, and studying the effects on the mechanical properties of the deposits proved to be areas of particular interest. Such results may be a harbinger of time savings as well as increased versatility in producing deposits.

FUNDAMENTALS

A schematic copper electrolysis cell would contain two electrodes submerged in an electrolyte and connected to a source of external voltage as shown in Figure 1. Without any externally applied EMF no net current will flow across the cell as the potential difference between the two electrodes is zero. In quasi-reversible conditions where only an infinitesimal current flows, and

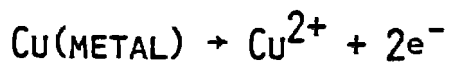
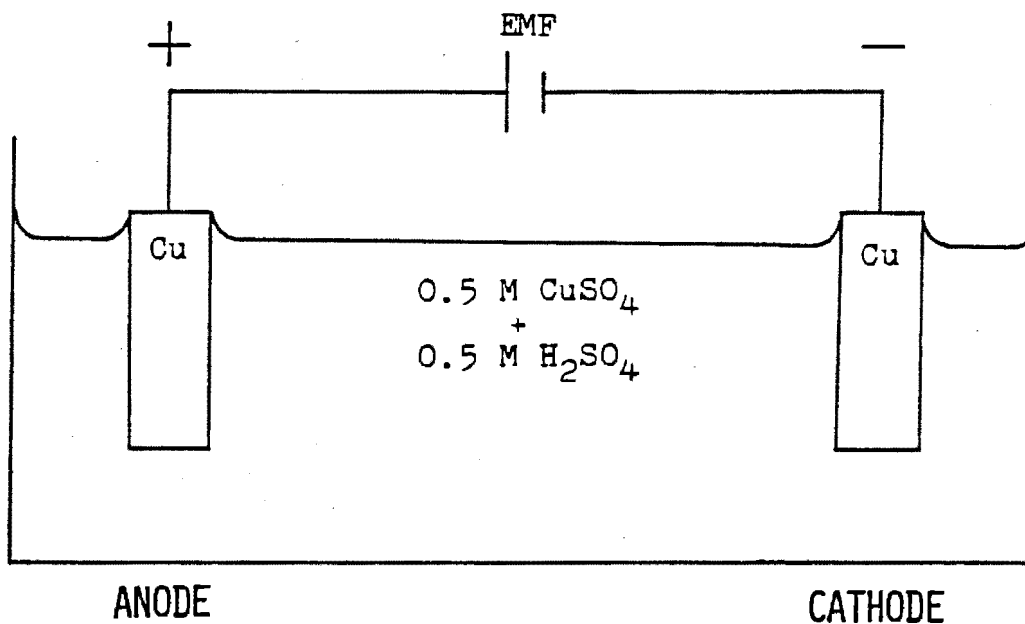


Figure 1. Schematic diagram of a typical copper deposition cell showing the electrodes, current source, electrolysis solution, and electrode reactions.

the electrode reactions can maintain equilibrium, the electrodes would maintain their reversible potentials (4, p.184). However, as Potter (5, p.124) notes, no electrode reactions can proceed reversibly from reactants to products, so once any appreciable and useful amount of current begins to flow an increase or decrease in the electrode potential occurs. This change in potential depends upon whether the electrode takes on an anodic or cathodic potential, respectively. This deviation from reversibility caused by the polarization of the electrodes is quantified by the overpotential. The greater the current the greater the irreversibility (5, p.124). This overpotential is the conglomeration of three distinct types of polarization as shown in Figure 2. The observed cell voltage (the voltage which must be supplied for the reaction to occur) is also a direct consequence of this polarization. Therefore, the trick is to keep the voltage as low as is possible and still obtain the desired result. In other words, one tries to avoid polarization and reduce the overpotentials as much as is practical (6, p.1052).

The interphase region. The region where the solid metal and the liquid electrolyte meet is the area of greatest interest. The metal electrode is made up of positive ions and free electrons. Moving into the electrolyte, we first encounter a layer of mostly water molecules which constitutes the solvation sheath. The

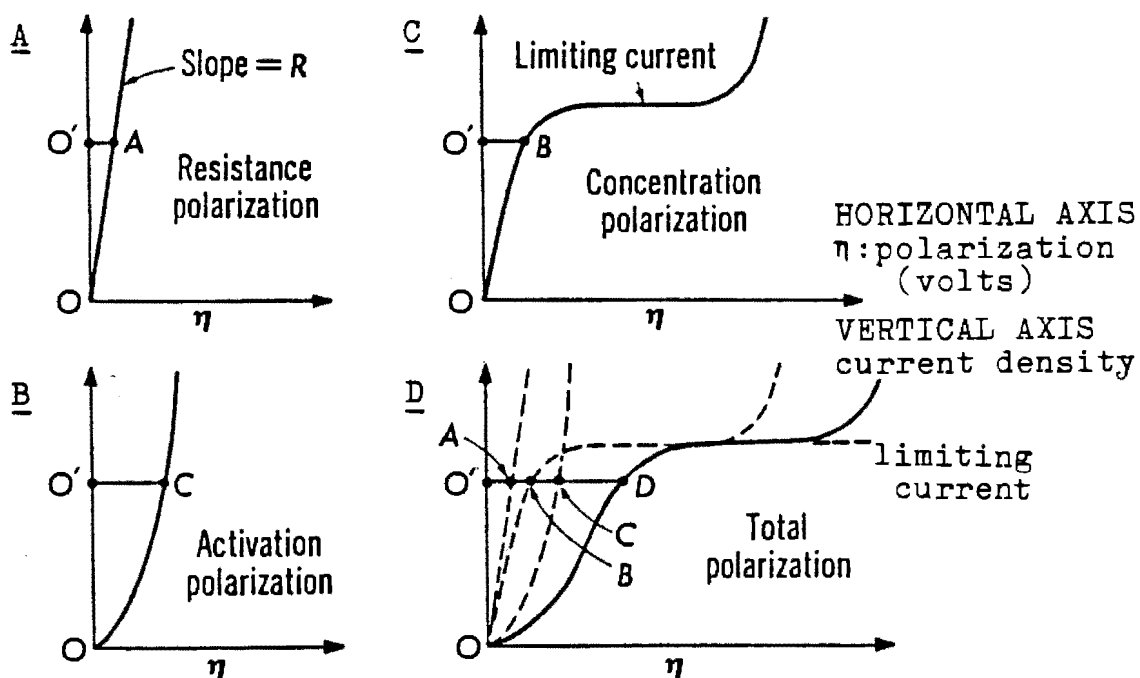


Figure 2. "Schematic representation of polarization types. Total polarization is the sum: $O'A + O'B + O'C = O'D$. (In practice, total polarization is observed, and the contribution made by the various types must be determined.)" **A**: ohmic **B**: activation **C**: concentration **D**: total (7, p.65)

second layer consists of hydrated copper ions, and the locus of the center of these ions is the outer Helmholtz plane. The so-called double layer is made up of these hydrated copper ions and excess electrons on the electrode. This description is significant in a hypothetical sense since in practice both positive and negative ions can become adsorbed onto the electrode surface. Much of the voltage drop for a cell occurs in this interphase region which is on the order of 10 Angstroms in thickness. Thus for a one volt drop which might typically be found in electrolysis, an electric field of 10 volts/cm exists in the interphase region (6, p.855).

Contributors to the cell potential and their effects

The ohmic or resistance polarization in an electrolysis cell is dependent on the nature of the electrolyte as well as the concentrations and equivalent conductances of the constituent ions in the solution (5, p.142). If only a small current is flowing so that the ion transport processes keep up with the production and deposition of ions (that is, no build up or depletion of ions or charge occurs) then ohmic and some activation polarization are the only significant contributors to the observed cell potential before other types of polarization begin to contribute to the overpotential. Ohmic

polarization increases linearly with increasing current as is indicated in Figure 2, A. As the applied potential is increased the activation and concentration polarizations become more apparent.

The activation polarization is related to the energy which the ion must possess, in excess of the average ion potential, in order to overcome the activation energy barrier for a reaction (7, p.53). The copper ions by thermal fluctuations must deform the hydration sheath enough to be in contact with the electrode surface. The reactions which occur at the electrodes, as can be seen from Figure 1, are the oxidation of copper to copper in the doubly ionized state at the anode and the reduction of the copper ion at the cathode with the subsequent transformation into an atom of stable metallic form. Because the reactions only occur at the electrodes the activation polarization occurs near the electrodes. The number of ions with sufficient energy to surmount this barrier is governed by the temperature and free energy of the individual ions as well as the height of the energy barrier (5, p.136). By increasing the temperature or increasing the electrode potential this energy distribution can be shifted towards higher energies, so that a greater number of atoms exist which have sufficient energy to react. Typical behavior of the activation overpotential is seen in Figure 2, B.

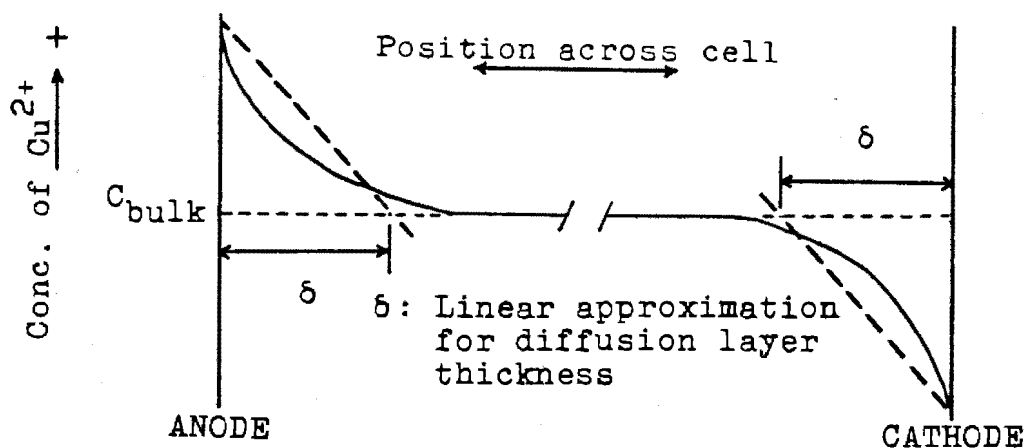
The transport processes which are operative during electrolysis are diffusion currents occurring very near the electrode, i.e. in the diffusion layer which is on the order of microns in depth (4, p.197). These currents are due to the concentration and/or activity gradients set up at the electrodes as the applied EMF is increased. Migration involves the effect of an applied electrical potential on the random thermal motion of the charge-carrying ions. Convection involves either a thermal or a density gradient. Stirring is one transport mechanism which can be directly controlled by the observer, and devices used to stir a solution would include mechanical systems such as an impeller or, as in this study, an external magnetic field superimposed on the electrolysis current.

As atoms from the metal electrode are ionized and go into solution at the anode, and deposition reactions occur at the cathode, there is a gradual accumulation of ions at the anode and a depletion of ions at the cathode. This change in local copper ion concentration occurs if the usual transport processes including diffusion, migration, convection and stirring are not sufficient to maintain the bulk-solution concentration of metal ions in the diffusion layer near the electrodes. As the concentration of positive ions increases near the anode and the concentration of positive ions decreases at the cathode

there is produced an additional contribution to the observed cell potential as shown in Figure 3. This is called the concentration overpotential, and in the case of copper electrodeposition where the activation overpotential is thought to be fairly small, the concentration polarization accounts for much of the electrode polarization at current densities above 10 mA/sq cm (5, p.130). Thus, the applied voltage must be sufficient to overcome this additional energy barrier. The behavior of the concentration polarization is shown in Figure 2, C. Ultimately, there arises a condition where the transport processes mentioned above can no longer transport any more charge even with an increase in the applied EMF. When this occurs, the limiting current has been reached.

The limiting current is the barrier which limits the rate of copper electrodeposition. The limiting current is shown in the Figure 2, C and D. No increase in the applied potential can cause an increase in the cell current until the overpotential is great enough for another reaction to commence. This secondary reaction is hydrogen gas production in the copper electrodeposition system. In any case, even with an increased current the desired copper reaction rate cannot be increased, and energy is wasted on hydrogen gas production at these higher current densities.

A. Concentration of Cu^{2+} vs. Distance across cell



B. Change in cell potential due to change in ion concentration vs. Distance across cell

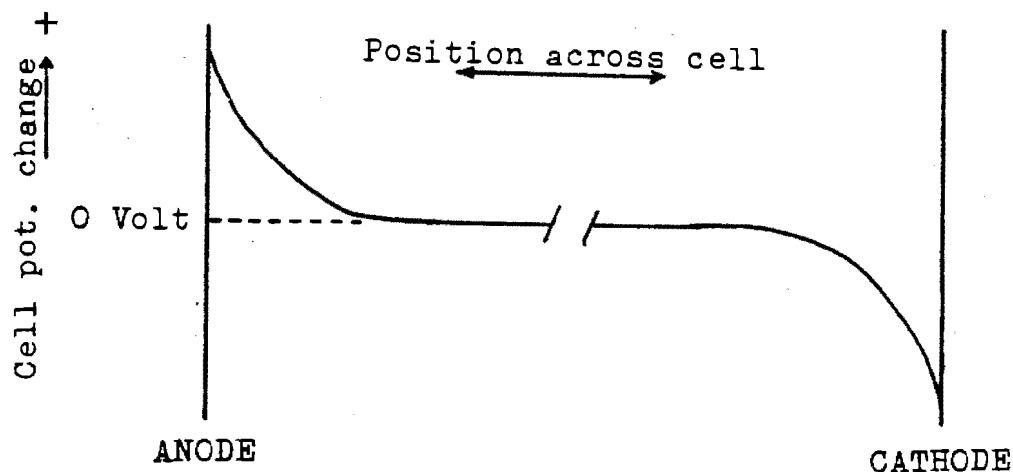


Figure 3. How concentration polarization appears as copper ion concentration in the region near the electrodes changes from the ion concentration in the bulk. Graph A shows the change in the ion concentration at the electrodes. Graph B shows the change in the potential at the electrodes. This potential change within the cell opposes the applied EMF.

Additional influences on electrodeposition

Stirring. As might be expected external stirring greatly increases the amount of metal ions brought to the cathode for electrodeposition. Why then should one be interested in magnetically induced stirring as opposed to mechanically induced stirring? Mechanical stirring definitely increases ion transport in the bulk solution, thereby delaying the onset of concentration polarization. However, mechanical stirring will tend to be damped out in the diffusion layer due to viscous effects and can have no effect on layers of electrolyte adsorbed onto the electrode surface. This is because the flow velocity at the solid-liquid interface for externally induced flow must be zero. On the other hand, the magnetic stirring effect can occur wherever there are charged particles in motion with an applied magnetic field. This means that a significant stirring effect can perhaps be obtained even in the diffusion and Helmholtz layer directly next to the metal electrode surface. The magnetic stirring occurs because of the Lorentz force on moving charged particles,

$$\vec{F} = Q (\vec{v} \times \vec{B}) + Q \vec{E}.$$

Where \vec{F} is the Lorentz force, Q is the charge on the particle, \vec{v} is the velocity of the particle, \vec{B} is the magnetic field and \vec{E} is the electric field. Curiously, in magnetic stirring no work is done on the charge carriers

since the magnetic force is always perpendicular to the velocity vectors of the charged particles.

Mohanta and Fahidy (8) have reported this magnetic stirring effect for electrolysis in flow cells inside a magnetic field. In their work, the electrolyte is mechanically pumped with the intention of increasing transport of ions in the bulk, and the electrolysis is performed in a magnetic field in order to augment ion transport in the diffusion layer.

Diffusion layer and diffusion. The diffusion layer is the region near the electrode where a concentration gradient exists such that transport of ions is driven by the gradient in addition to possible electrical effects. Mechanical convection is not considered in the diffusion layer since externally induced stirring is usually damped out near the electrode. Also where convection or agitation currents are operative, the ion concentration tends to remain near the bulk-concentration so that the concentration gradient is altered (9, p.132)

The diffusion rate is controlled by Fick's law which is

$$i = \frac{n F D (C_b - C_e)}{\delta}$$

where i is the diffusion current, n is the number of electrons necessary for one reaction to occur, F is Faraday's constant (94500 C) which is the charge in one

mole of electrons, D is the diffusion coefficient, C_b is the ion concentration in the bulk, C_e is the ion concentration at the electrode surface, and δ is the diffusion layer thickness. As shown in Figure 3, a linear approach is often used to approximate the thickness of the diffusion layer.

The diffusion layer thickness is on the order of 0.5 mm or less for non-agitated solutions, but may be one to two orders of magnitude smaller for a mechanically stirred solution (9, p.200).

If the reaction rate is controlled by the activation-potential barrier and concentration overpotential is relatively low then the reaction is under potential control (9, p.126). In such a case, the current density is likely to be low and there are plenty of ions available at the cathode which cannot overcome the barrier. If a reaction is under diffusion control, then the rate determining process is the transport of ions to the electrode. At high current densities and high concentration polarizations the cathode reaction is under diffusion control, and it is advantageous to make the diffusion layer as thin as possible.

Magnetoresistance. Although the magnetic stirring effect may decrease the concentration overpotential, there are effects which may increase the resistivity of the solution. The Lorentz force on the charge carrying ions

deflects them from their usual paths. This deflection hinders the movement of ions to the electrodes since the ions are subject to a force perpendicular to the applied electric force. The effect of the magnetic force also sets up an additional electric field which is transverse to the applied electric field. Such a transverse electric field would also alter the usual motion of the charge carriers. The polarity of this additional Hall electric field depends upon the polarity of the charge carriers. Since both positive and negative ions are present, one might expect that the respective Hall electric fields will effectively cancel. However, a net effect is reported and explained by Laforge-Kantzer (10) who points out that the mobility of protons (hydrogen ions) is significantly greater than other ionic species found in common acidic electrolyte solutions. Because of this large difference in the velocities of the ions a net "ionic" Hall effect is observed. Read and Katz (11) also write, "the ionic Hall effect arises from the action of the magnetic field on the asymmetry in the motion of the ionic charge carriers set up by the applied electric field." Cousins (12) reports a net decrease in the cell voltage when electrolysis is performed in a magnetic field as compared to no applied magnetic field although the effect of this "magnetoresistance" is also recorded.

CHAPTER II

THE EXPERIMENT AND ANALYSIS

EXPERIMENTAL APPARATUS AND PROCEDURES

A simplified view of the apparatus used in the experiments is shown in Figure 4. The cell (43 mm H X 22 mm ID, 2 mm glass thickness) used in experiment runs 2 to 69 was fabricated from a brown glass medicine bottle by cutting off the threaded top portion. In experiment runs 70 to 116, a glass cell (69 mm H X 33 mm ID; jacket 75 mm H X 102 mm OD) with a cooling jacket was used. A Harrison HP-6202B DC power supply (PSU#43130, SN6K2046) provided the electrolysis current regulated constant to at least ± 1 mA in the range 0 to 750 mA with a 40 V maximum. Currents up to 880 mA were also obtained with only a 1% variation although this is outside the guaranteed regulating range. The electrolysis current was set using a Fluke 853A Differential Multimeter (PSU# 42335; $\pm 0.2\%$ reading + 0.02% range). Fluctuations in electrolysis current were detected with the differential multimeter and computer read-out. The current densities were between 80 mA/sq cm and 880 mA/sq cm.

The solution used in the deposition experiments contained 0.5 M CuSO_4 and 0.5 M H_2SO_4 in deionized water.

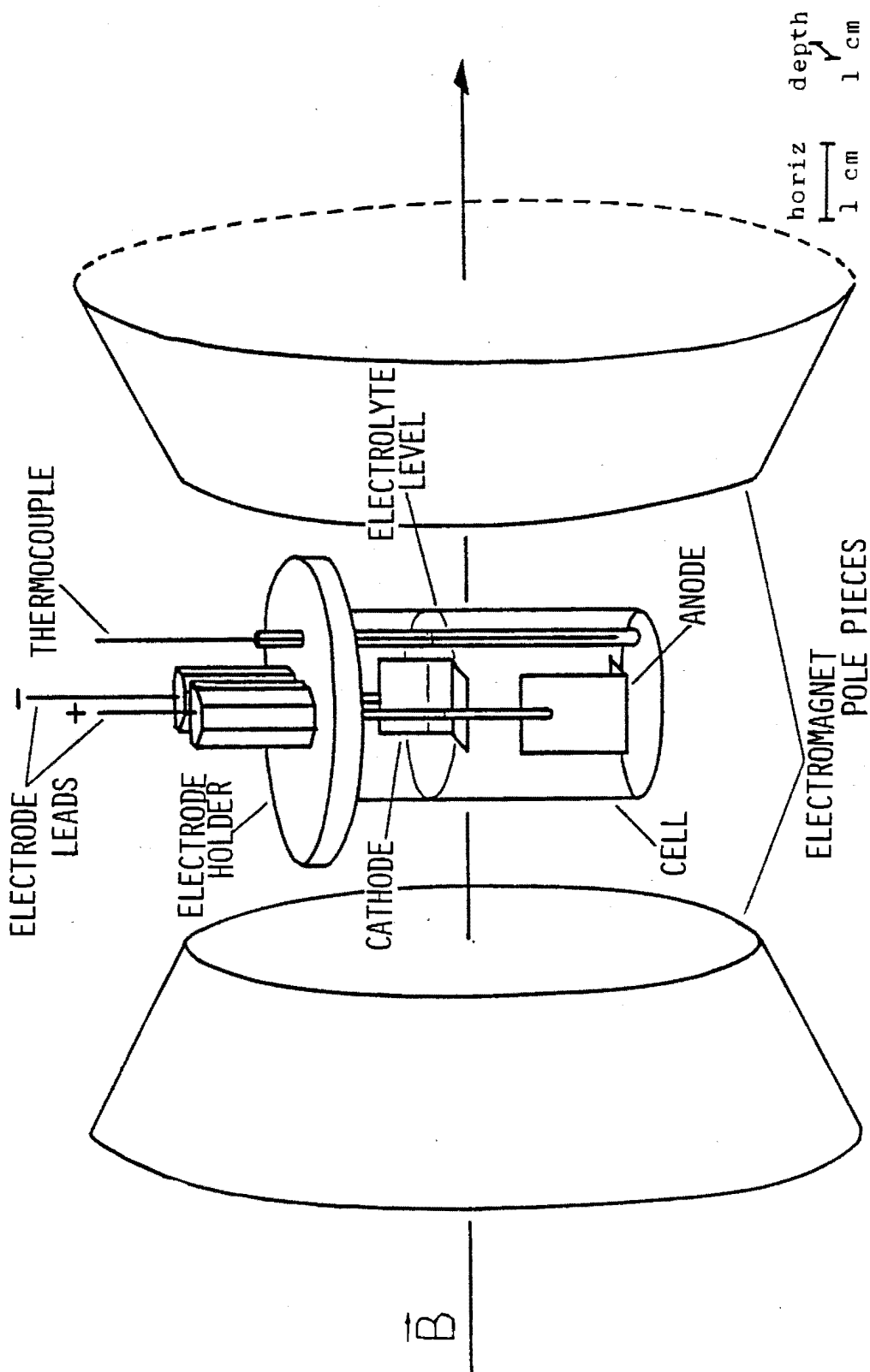


Figure 4. Diagram of cell without a water jacket used for copper electrodeposition experiments showing alignment of magnetic field. The copper electrodes are fastened with screws or clamped to the leads. The water-jacketed cell is set up similarly.

This electrolyte was mixed prior to the beginning of the experiments and stored in a brown glass bottle. Although the solution inside the cell was not changed following each experiment, the level of the electrolyte was maintained to submerge all of the cathode surface by 3 mm. Therefore if the solution level appeared to be too low after inserting the electrodes directly before an experiment, then just enough solution was added with a Pasteur pipet. The solution was changed and new solution placed into the cell only when an accumulation of copper powder appeared on the bottom of the cell.

A Chromel-Alumel thermocouple connected to an Omega Cold Junction Compensator (published precision of ± 0.25 degrees Centigrade) monitored the temperature of the bulk solution in the cell. The thermocouple was placed in a glass capillary tube, with the bottom sealed off by melting, in order to protect the thermocouple from the electrolyte. The tube and thermocouple were then situated along the inside wall of the electrolysis cell with the spot welded tip of the thermocouple about 0.5 cm from the bottom of the cell.

In our earlier experiments (run 2 to 69), the temperature control was achieved with the aid of the cooling water to the magnet. By maintaining a flow of cooling water to the magnet coils it was possible to obtain a temperature of 15 deg C with a current density of

80 mA/sq cm. The temperature of the water used for cooling was affected by ambient conditions making our task of maintaining a constant temperature quite difficult especially with the changing of the seasons. Also, temperature control was poor when using higher current densities. When the cell with the temperature-controller water jacket was connected to the Bayley Instruments Co. Model 325 temperature-control bath control to within ± 0.2 deg C was possible. A Cole-Parmer pump forced the constant-temperature water through the tubing and around the cell. This latter cell was chosen in hopes of improving the temperature reproducibility, and in this regard, proved to be successful. However, the unjacketed cell, although lacking a dependable temperature-control system, offered the advantage of a smaller diameter making it possible to apply greater magnetic fields to the cell during electrolysis.

A Varian V-4004 water-cooled electromagnet with a Varian V-2301A power supply and V-2300A current regulator provided the magnetic field in the range 0.11 kG to 12 kG with 3 inch pole pieces and up to 12.5 kG with 2 inch pole pieces (both with a gap of 27 mm which was used with the smaller-diameter-cell set-up). The electromagnet produced a magnetic field in the range of 0.073 to 0.74 kG with 3 inch pole pieces and a 55 mm gap with the larger diameter cell. The ripple in the magnetic field is documented to

be one part in ten thousand, and with the current regulator operating, the fluctuation in the magnetic field is one part in one thousand for a ten percent variation in the load resistance or line voltage. The magnetic field was measured using a Bell 620 Gaussmeter (PSU# 43292). The magnetic field varied about 0.2 kG from the center of the field to the edge of the pole piece at 7.40 kG. At lower magnetic fields the field was constant to about 7% over the entire region between the pole pieces. The magnetic flux density for the cell placed in a holder outside the magnetic pole pieces was 2.8 Gauss or 0.0028 kG which is about five times the earth's magnetic field in our laboratory. This cell was used in the experiments where the magnetic field is indicated as "0 kG" or "outside."

The circuit diagram (Fig. 5) shows the set-up used in all the deposition experiments except for the temperature-control devices which were added later. Cell voltage, cell current, and cell temperature were monitored and recorded with the aid of an Aim 65 Microcomputer system developed and programmed by C. Cousins.

The substrate material for the electrodes was an electrical buss bar material (C11000, at least 99.9% copper) and a desired length was cut from this stock rod. After cold rolling the copper until cracks formed along the edges (about 3 mm thickness) with the Denver Fire Clay

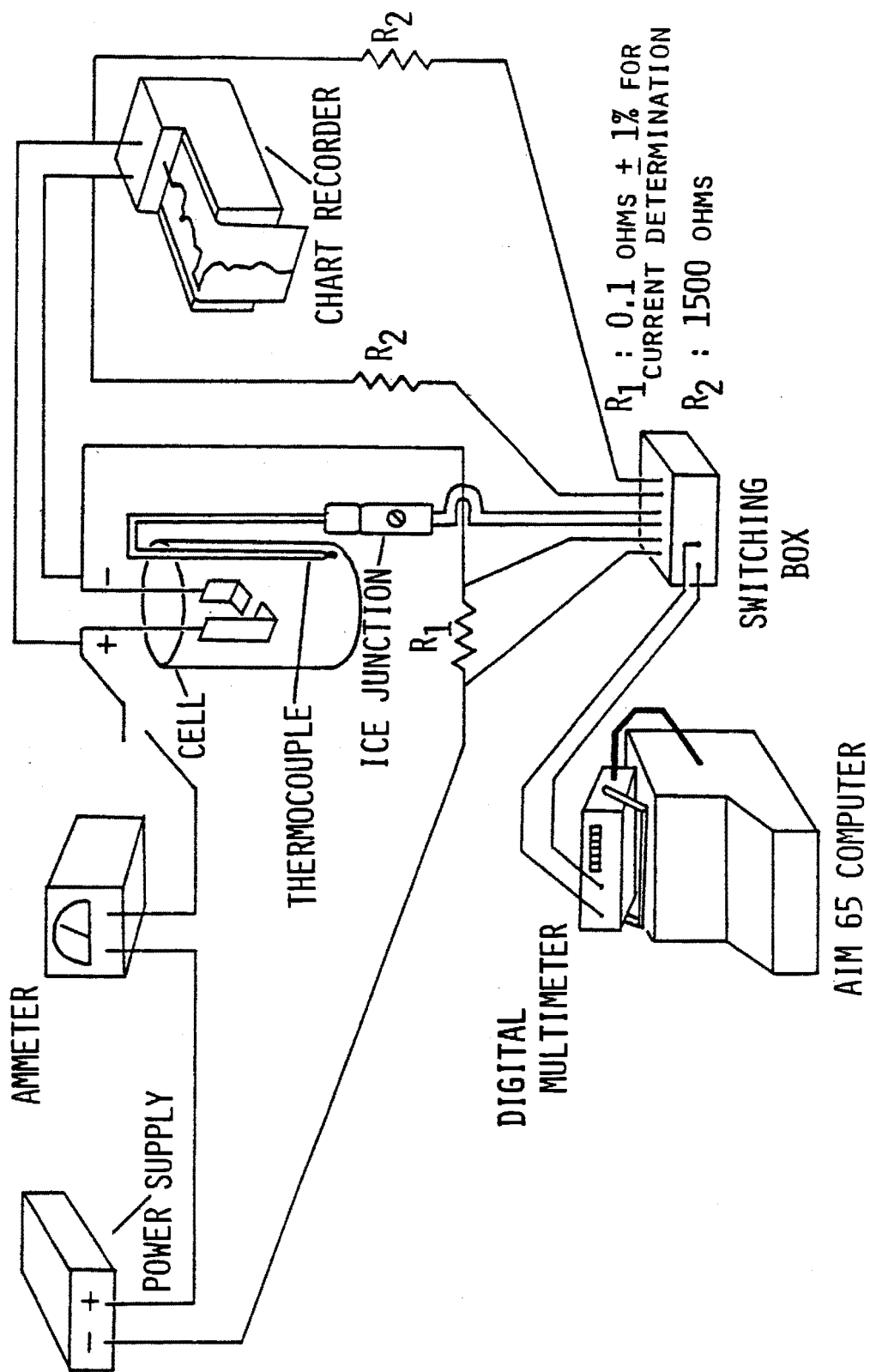


FIGURE 5. DIAGRAM OF EXPERIMENTAL SET-UP (NOT TO SCALE). MAGNET NOT SHOWN.

cold roller (PSU# 50480), the sample was annealed at 1300 degrees Fahrenheit (700 deg C) inside a Thermolyne metallographic oven in ambient atmosphere for 5 minutes and quenched in ethanol or methanol which provided a relatively reducing atmosphere in order to reduce the amount of oxidation. Another anneal was done when cracks again began to form along the edges (about 0.5 mm thickness) and a final anneal (at about 0.25 mm thickness) completed the rolling process. The layer of copper oxide which forms on the copper surface is removed by sanding with 320 grit silicon carbide sand paper, and the strips of copper are then chemically polished in a solution containing 1/3 nitric acid, 1/3 glacial acetic acid, 1/3 orthophosphoric acid by volume heated to at least 70 deg C. The copper strips were washed with tap water, then rinsed with deionized water and then rinsed with acetone and air dried. The final thickness of the electrode material varied between 0.15 mm and 0.20 mm depending upon how much sanding and polishing was done. Generally, the thicker material was chosen for the anodes. The thickness of the electrode material was chosen because of the ease in cutting and bending. The strips were then cut into 1 cm wide sections which subsequently were cut to lengths of 4 cm for anodes and 2 cm for cathodes. The strips were bent at a point 1 cm from one end so that a 1 sq cm area surface (horizontal part) was produced at a 90 degree

angle to the remaining part (vertical part). Numbers were inscribed on the vertical part with a diamond tipped scribe. The electrodes were covered with two or three coats of Microstop, an acetone base plastic paint, in order to insulate the copper surface from the electrolyte where copper deposition or dissolution were not desired. On the cathode, the entire vertical portion and the top surface of the horizontal portion were painted providing a total unpainted (exposed) surface area of 1 sq cm. On the anode, just the vertical portion was painted, resulting in a total exposed surface area of 2 sq cm. These electrodes were then stored away in covered glass petri dishes until use.

Typically, a day of experiments started out with the turning on of the equipment and meters. The digital Fluke meter and the strip chart recorder were kept on over extended periods when experiments were being performed because of the lengthy times required for these instruments to stabilize. The temperature-control bath requires at least 30 minutes to stabilize after switching on and setting the control dials. In the meantime, the computer was provided with the appropriate program from a cassette and placed in the proper mode to monitor the experiment. A cathode and anode were chosen out of the stockpile and weighed on a Mettler H80 precision balance. After weighing, the electrodes were fastened onto the

electrode holder and positioned to lay directly over each other with the desired gap (usually 2 cm) separating them. If a magnetic field is to be used, the magnet-coil cooling water was turned on, and the current regulator was allowed to warm-up. The electrode holder was inserted into the cell, and the electrode leads were attached. A final check of the positioning and electrolyte level was performed before switching on the magnet-coil current. The meter settings were checked, the chart recorder paper switched on and finally the electrolysis current turned on. Any small adjustments of current were made and the meters and computer were monitored to assure proper functioning. At the desired time the electrolysis current is shut off, the magnet current shut off and the electrodes are removed from the cell. The electrodes are immediately rinsed with deionized water, then methanol, and finally blown-air dried. The anode and cathode were weighed in order to find the mass gain or loss.

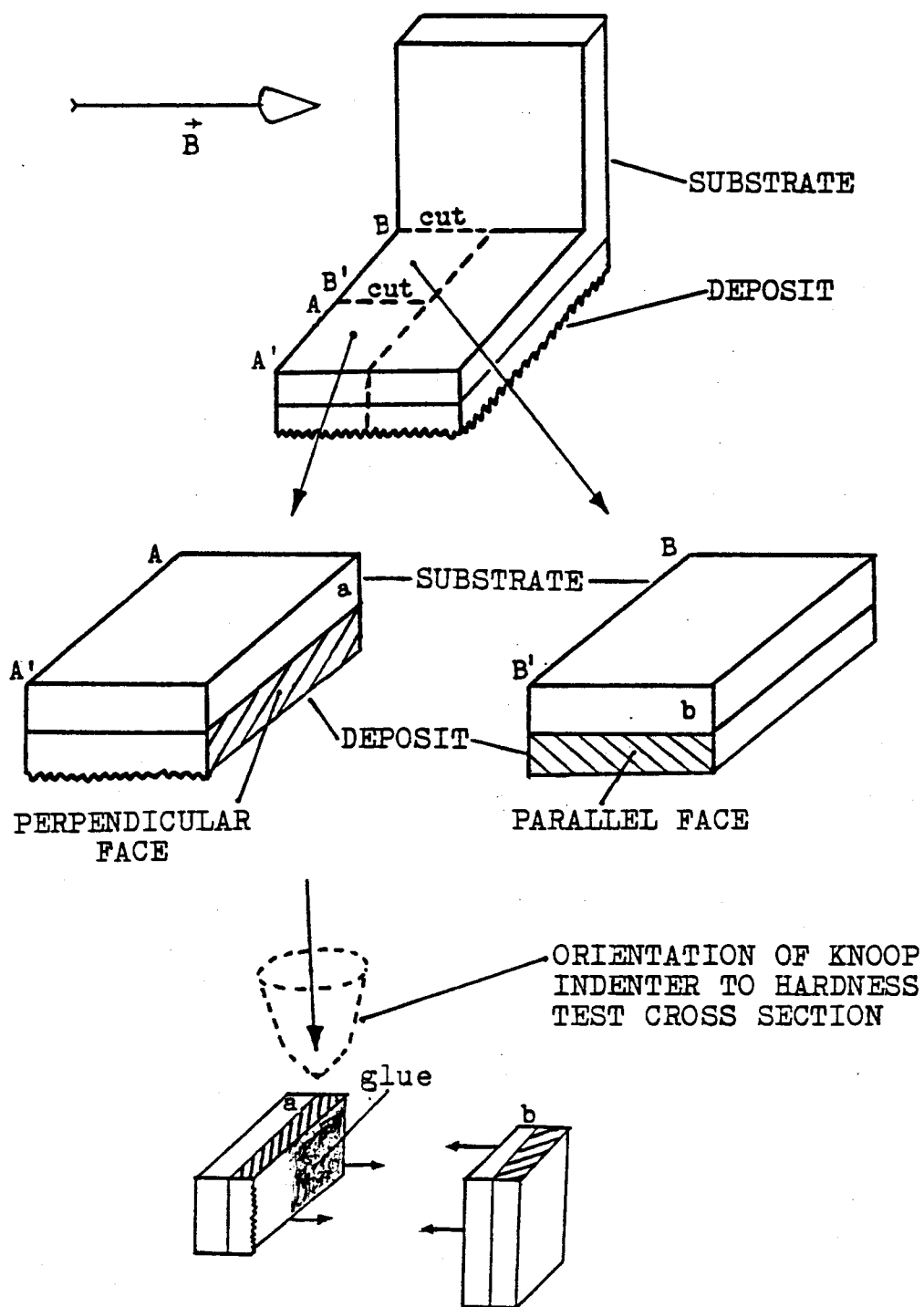
For ease in comparison, each experiment was continued until 144 coulombs of charge were passed. The thickness of the deposit for a 1 sq cm area is about 50 microns.

ANALYSIS

Hardness testing. A Tukon Tester provided Knoop hardness information which served as a measure of mechanical properties. Knoop hardness measures wear and abrasion resistance and also can be used to compare strengths of the materials.

As preparation for hardness testing the specimens were cut so that one surface perpendicular to the magnetic field and one surface parallel to the field were produced as shown in Figure 6. These pieces were stuck together with super glue so that "perpendicular" and "parallel" surfaces would face out alternately. This row of specimens was mounted in Bakelite or "Electromet" conductive mounting compound both of which require heating to 150 deg C for 5 minutes at high pressure or "Plastimet" which simply requires the mixing of a powder with a setting liquid at room temperature. These mounts were ground with silicon carbide sand papers until a flat surface was achieved. After grinding, the mounts are polished with 3 micron diamond compound or 0.3 micron alpha-alumina and then 0.05 micron gamma-alumina to a lustrous finish. Following the final grinding stage and between the polishing stages, the mounted specimen was ultrasonically washed with Labtone soap. It was rinsed each time with tap water, deionized water, and methanol

Figure 6. Cross sectioning of deposit for hardness testing. Cathode faces are 1 cm x 1 cm area (not to scale).



THE SECTIONS ARE GLUED TOGETHER AND THEN MOUNTED.

then blown-air dried. The specimen was etched in a solution containing 1/3 orthophosphoric acid, 1/3 nitric acid, 1/3 glacial acetic acid by volume until the crystalline grains could be made out clearly with a light microscope. This required an etch of about 15 to 20 seconds at room temperature. The mounted and etched specimens were kept in covered petri dishes for storage.

Five indentations spaced roughly equally apart were made on each deposit and substrate material where possible. Each test was conducted with a load of 50 gm and with the 50X objective lens in place. At the same time, we observed how grains from the substrate appeared to grow into the deposit and the prevalent grain size of the deposits.

Microscopy. The scanning electron microscope (SEM; ISI-SS40, PSU# 59033) and the Reichert-Zetopan metallographic light microscope (SN328904, PSU#41119) became valuable tools in our study of the surface morphology and cross section characteristics. The SEM was particularly effective in providing a very clear view of the surface.

CHAPTER III

EFFECT OF AN APPLIED MAGNETIC FIELD ON LIMITING CURRENT AND DEPOSITION ENERGY

As previously mentioned, the existence of the limiting current limits the rate of deposition possible. As polarization increases and the limiting current is approached, it becomes steadily more difficult to pass current through the cell and to increase the copper deposition rate. More and more energy is required to overcome the additional polarization which arises as the current is increased. Barring a change in the resistivity of the solution or an increase in the activation overpotential, the extra applied potential goes into overcoming the concentration overpotential. This energy goes into Joule heating and into producing hydrogen and oxygen and is lost.

DEFINITION OF QUANTITIES

Deposition energy

The deposition energy (DE) provides a convenient means of comparing various plating conditions. It is defined as,

$$DE = \int_0^{t\text{-final}} J \times A \times V(t) dt$$

where J is the apparent current density, A is the apparent cathode area, $V(t)$ is the cell potential at time t and t -final is the length of the deposition run.

Method one. In actual practice the DE was found by two different methods. Method one utilized the cell voltage and coulombic data printed out by the computer every 30 seconds. The average of the beginning and ending voltage was found for each 30 second interval, and this value was multiplied by the total current passed through the cell during the interval. Thus,

$$DE = \text{average voltage} \times \text{total charge passed}$$

If large voltage fluctuations occurred as in the high current density (CD) experiments this method gave values significantly different from method two.

Method two. Method two was graphical and utilized the voltage versus time graph from the chart recorder. The chart record was conveniently made on a grided paper so that the area under the voltage curve was calculated by counting the number of squares. The number of squares is multiplied by the appropriate factor in units of volt-sec. The product of this result with the cathode area, A , and cathode current density, J , gives the DE.

$$DE = \# \text{ of squares} \times \text{volt-sec per square} \times A \times J$$

Thus, the DE is mostly a measure of the average cell polarization during a deposition run since the cell current density is maintained constant. Where the

polarization is small the average cell voltage will be smaller, and the DE will be lower. The increase in total surface area of the cathode with increasing deposit was not considered for this calculation although Mohanta and Fahidy (13) have reported that the rate of cathodic mass transfer can increase with increasing roughness of the deposit. Because of its thickness, the anode area decreased by as much as 5% in most experiments until a thicker anode material was chosen. Although the geometrical surface area was reduced, it should be mentioned that there probably was some increase in the actual effective surface area as the anode dissolved. This is because the anode surface which is initially shiny often takes on a more etched surface which exposes more surface area to the electrolyte. See Figures 10-14 and 17-20 (pictures of anodes and cathode). Actual measurements of the effective surface area were not undertaken.

Efficiency

A measure of whether the current was going toward useful plating or not was provided by the notion of "efficiency."

$$\text{Efficiency} = \frac{\text{Actual cathode weight change}}{\text{Expected cathode weight change for 144C passed}}$$

The expected weight change is calculated based upon the cathode reaction of



Therefore, if the parasitic reaction of hydrogen production is occurring, then the efficiency will be less than 100%. In addition, if the copper deposit is poorly adherent then small chips are lost into the solution or lost during specimen handling following the experimental run. In a spongy, loose deposit a 40-50% loss of deposited copper can occur during handling. These chunks were not collected and weighed since our primary interest is in obtaining a compact deposit. Near 100% efficiencies are therefore only seen in bright, compact, well-adherent deposits. 144 C was chosen since this is the amount of charge passed during a 30 minute period at 80 mA/sq cm current which were the conditions used in our earliest experiments.

The expected weight change (EWC) for the cathode is calculated as follows.

$$\text{EWC} = \frac{\text{Charge passed} \times 63.5\text{gm}}{2 \times 96500\text{C}}$$

where 63.5 gm is the atomic weight of copper. The factor of 2 must be included because two electrons are required to discharge the copper ion in solution to produce one metal

atom. 96500 C is one Faraday unit and gives the amount of charge in one mole of electrons.

In this fashion it is possible to determine if the limiting current for copper deposition is exceeded. Whenever the limiting current is exceeded, i.e. the transport processes cannot supply enough copper ions to the cathode for useful plating to occur, the efficiency will be low, and the deposition energy will be high because of the excessive concentration polarization. A deposit at such conditions would be spongy, dark-brown, and poorly adherent probably due to production of hydrogen during the experiment. If the efficiency was near 100%, we concluded that the limiting current was not exceeded, and the deposit was invariably compact and well-adherent. Bright deposits could be obtained until efficiency dropped to about 70% although at higher current densities ($> 400 \text{ mA/sq cm}$) some very rough deposits had 80 and 90 percent efficiencies if vigorous handling was avoided (with thorough cleaning $< 10\%$ efficiency). But whenever efficiency dropped below 50%, the result was a poor deposit, and hydrogen production was detected.

EXPERIMENTAL RESULTS AND DISCUSSION

Our results also show a change in the limiting current and the energy required for deposition. The results of experiments performed at 80 mA/sq cm current

density point out most clearly the claim that limiting current increases with the application of a suitable magnetic field.

Effect of the B field on the efficiency

Table I shows the results from a battery of experiments where the only varied parameter for any given CD was the applied magnetic field with the smaller non-water-jacketed cell. Table II shows similar data for experiments in the water-jacketed cell.

At the residual field strength of the electromagnet, i.e. no magnet current, but with the cell between the magnets, an efficiency of 77% is recorded, but this is due to special handling of the deposit in order to preserve the powdery deposit. Gas production was observed for the experiment performed at this lowest magnetic field strength. In normal handling procedures the deposit fell off readily when washed with deionized water following the experiment.

The deposit at 0.80 KG is an example of an easily removed deposit which results in an efficiency of 37%. At 1.55 KG, the current efficiency jumps to 93% and remains essentially constant up to 12.5 KG. Similarly at 160 mA/sq cm C.D the current efficiency finally approaches 100% at 10 KG. Results shown in Table III at higher current densities (190-880 mA/sq cm) show that higher efficiencies can be

TABLE I

LOWER CURRENT DENSITY EXPERIMENTAL DATA
SMALLER DIAMETER CELL WITHOUT WATER JACKET

RUN #	B KG	CD mA/sq cm	EFFICIENCY %	ENERGY J	AVG T deg C	T RANGE deg C
30	0.11	80.0	77	126	15.17	15.09-15.32
46	0.80	80.0	37	118	14.84	14.72-15.04
47	1.55	80.0	93	102	14.98	14.74-15.37
34	2.60	80.0	94	105	15.18	15.02-15.39
29	4.00	80.0	97	98	15.03	14.62-15.12
39	4.80	80.0	98	93	15.37	15.09-15.67
40	5.80	80.0	98	95	15.04	14.54-15.19
45	7.50	80.0	97	89	14.94	14.72-15.22
41	8.70	80.0	98	87	15.33	15.04-15.44
44	9.50	80.0	97	86	15.11	14.97-15.29
42	10.0	80.0	98	86	15.11	14.99-15.17
38	11.0	80.0	96	90	14.95	14.79-15.17
37	12.5	80.0	98	93	14.86	14.35-15.37
48	2.70	160	0	156	14.94	13.57-14.69
49	4.00	160	37	163	15.54	15.17-15.74
50	4.80	160	34	160	15.27	14.25-15.69
51	5.80	160	88	162	15.82	14.59-16.31
52	7.00	160	57	160	14.35	13.57-14.69
53	8.10	160	73	155	14.92	14.45-15.12
57	10.0	160	98	150	14.57	13.60-15.04

TABLE II

LOW CURRENT DENSITY EXPERIMENTAL DATA
 CURRENT DENSITY = 80.0 mA/sq cm
 LARGER DIAMETER CELL W/TEMPERATURE CONTROL BATH

RUN #	B KG	EFFICIENCY %	ENERGY J	AVG T deg C	T RANGE deg C
111	out	59	85	15.39	15.37-15.42
110	0.074	88	93	15.46	15.44-15.54
71	0.55	98	87	15.53	15.49-15.54
72	0.95	98	86	15.57	15.54-15.62
73	1.40	98	66	16.01	15.99-16.01
103	1.40	97	76	15.40	15.39-15.44
74	1.80	97	68	16.04	16.01-16.14
75	2.20	98	65	16.03	16.01-16.06
94	2.80	98	75	14.91	14.89-14.94
96	3.20	98	72	15.42	15.39-15.47
97	3.20	99	71	15.43	15.42-15.49
95	3.60	98	77	not recorded	
70	4.20	96	76	15.42	15.37-15.57
76	4.20	97	69	16.03	16.01-16.06
98	4.80	98	70	15.40	15.39-15.44
99	5.50	96	71	15.59	15.27-15.94
100	6.00	99	75	15.54	15.52-15.57
101	6.50	98	74	15.51	15.49-15.54
102	6.90	99	73	15.50	15.49-15.54
77	7.40	98	68	16.01	15.99-16.04

TABLE III

HIGH CURRENT DENSITY EXPERIMENTAL DATA
MAGNETIC FIELD = 7.4 KG
LARGER DIAMETER CELL W/TEMPERATURE CONTROL

RUN #	CD mA/sq cm	EFFICIENCY %	DEPOSIT C-compact NC-non-comp.	ENERGY J	AVG T deg C	T RANGE deg C
78	190	100	C	122	16.67	15.87-19.27
80	190	100	C	114	16.04	15.97-16.06
104	240	79	C	135	16.13	16.09-16.16
81	250	missing	C	148	16.08	15.99-16.11
112	300	88	C	177	15.67	15.42-15.77
83	320	97	C	970	17.09	16.01-18.48
113	320	72	C	194	not recorded	
114	340	68	C	205	15.66	15.59-15.59
115	360	94	N C	208	15.72	15.59-15.77
84	380	91	N C	249	15.99	15.92-16.06
105	420	81	C	1820	not recorded	
117	420	5*	N C	1800	17.46	15.54-18.85
85	480	76	N C	2530	not recorded	
86	480	79	N C	2430	19.25	16.16-23.35
106	480	missing	N C	1950	19.21	15.99-23.07
87	560	72	N C	3040	20.73	16.41-24.04
107	560	77	N C	2250	not recorded	
88	640	97	N C	3080	20.96	15.87-24.46
91	710	98	N C	3100	20.66	15.34-23.57
89	720	86	N C	3400	19.97	15.29-22.75
90	800	missing	N C	3300	not recorded	
92	800	missing	N C	3140	22.00	15.39-25.97
108	800	92	N C	2970	21.91	16.06-25.80
93	880	missing	N C	3010	21.90	15.39-25.23
109	880	97	N C	2710	22.31	16.11-25.30
116	880	5*	N C		not recorded	

* Sprayed vigorously with deionized water. No mechanical abrasion used.

achieved at some higher C.D.'s. Basically, it is possible to obtain a bright, adherent deposit just by applying a suitable magnetic field at some higher CD's. Furthermore experiments 85 and 106 were performed with a 1 cm gap between the electrode surfaces, and experiments 107-109 and 86-89 had a 5 mm gap between the electrodes. This decrease in gap width decreases the ohmic polarization by decreasing the distance through which the charge must migrate. However, the activation and concentration polarizations should not be greatly affected since the latter two phenomenon are primarily diffusion layer and electrode effects. This shift from our standard procedure occurred because with the wider gap the maximum regulating voltage for the power supply was being exceeded. Furthermore, the change was made in the interests of safety. In actual practice, little variation was seen by reducing the electrode gap at these higher current densities.

The deposits at current densities above 340 mA/sq cm were found to be rough and powdery except Run 105 at 420 mA/sq cm which was not reproduced. The high efficiency values occurred because vigorous cleaning was not performed. When the cathode was thoroughly cleaned a 5% efficiency was found.

DE versus applied B field

The graph of energy versus applied magnetic flux

density (Figure 7) shows how the energy of deposition is affected. At 80 mA/sq cm, the effect is quite dramatic. The highest recorded energy for deposition was 148 J outside the magnetic field varying down to 127 J. The DE falls to 80 J at 10 kG which was the lowest value recorded. After 10 kG, the the DE again tends to rise upward. Also shown in the same figure are the DE's taken at 160 mA/sq cm. Not as large an effect is seen at the higher current density. This data was taken with the smaller electrolysis cell without the temperature controller.

The energy obtained from the latter experiments performed in the water-jacketed cell are shown in Table II for a CD of 80 mA/sq cm. No great variation is seen with respect to applied magnetic flux density. The deposits produced at an applied magnetic flux density of less than 1.4 kG were not compact and the deposition energies are in the 80 J range. At 0.55 and 0.95 kG the deposits were too rough to make hardness measurements even though their corresponding efficiencies are high.

With the larger cell diameter it is likely that the flow of electrolyte was not as strongly damped as with the smaller diameter cell. Damping of the electrolyte flow may occur due to interaction of the solution with the cell walls or electrodes through the viscosity of the fluid. Reduction of the concentration overpotential in the larger cell may be accomplished at fairly low magnetic fields, so

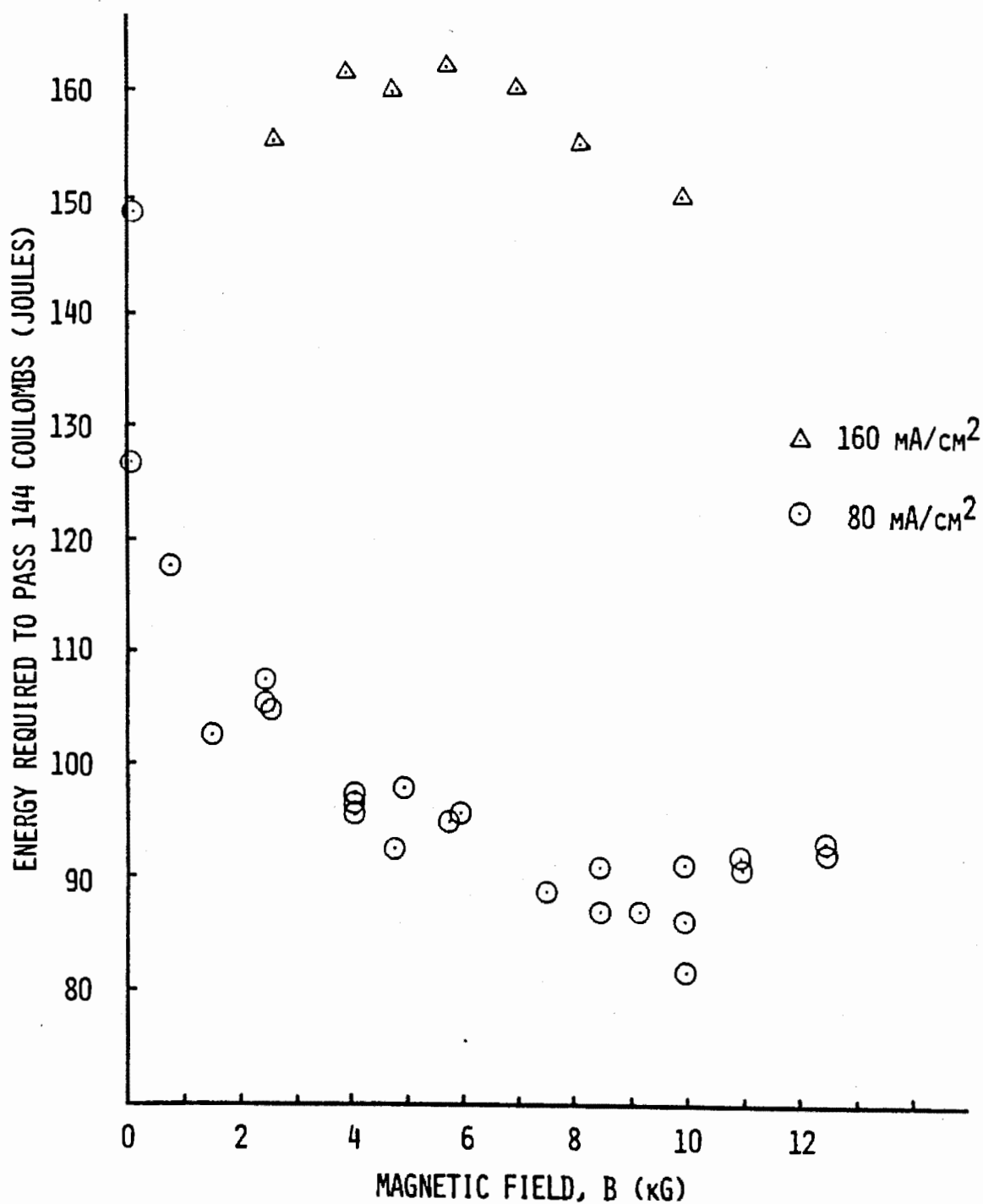


Figure 7. Effect of a magnetic field on energy of deposition. The energy data from Table 1 is plotted. The smaller diameter cell without a water jacket was used.

that the electrolysis comes under activation potential control as opposed to diffusion control.

At C.D.'s above 160 mA/sq cm, compact deposits could be obtained up to about 320 mA/sq cm with an applied field of 7.4 KG. The 970 J DE found for run 83 remains unexplained and appears to be a fluke because it is so radically different from the neighboring values. Otherwise the DE makes a dramatic jump at 420 mA/sq cm, and thereafter remains in the 2000 to 4000 J range up to 880 mA/sq cm.

The typical voltage versus time characteristics at 80 mA/sq cm are shown in Figure 8, A. For CD's higher than 160 mA/sq cm the voltage curves are similar to the lower current density (80.0 mA/sq cm) voltage-time characteristics up to 420 mA/sq cm. After a sharp increase in the cell potential when the power supply is turned on there is a gradual drop as deposition continues. The cell voltage versus time graphs shows a rapid increase which at a chart recorder speed of one inch per minute makes a vertical line. The voltages for the experiments performed at 80 mA/sq cm were around 0.5 volts. After the rapid rise the voltage immediately begins to taper down gradually. The voltage decrease from start to finish of an experiment is usually about 0.05 volts.

However, for CD's of 420 mA/sq cm and above the voltage-time characteristics are more like those shown in

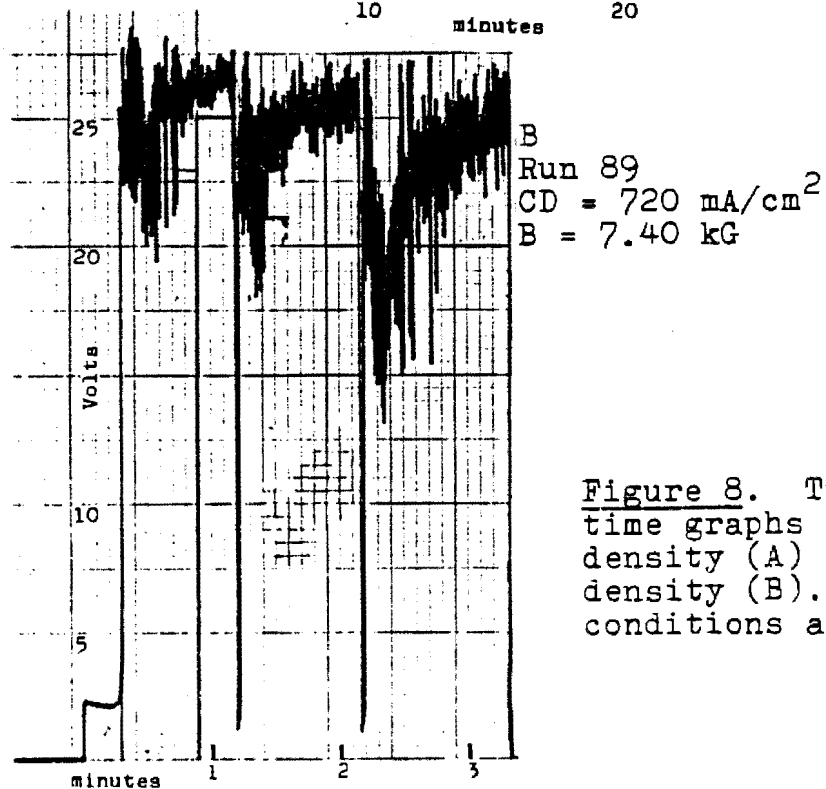
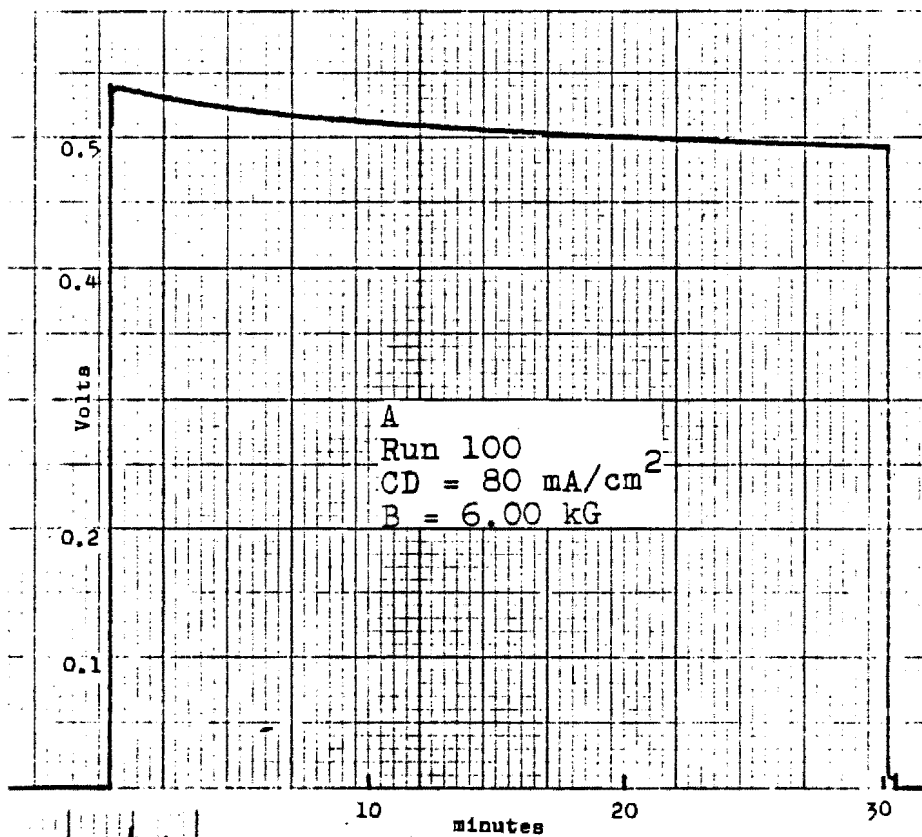


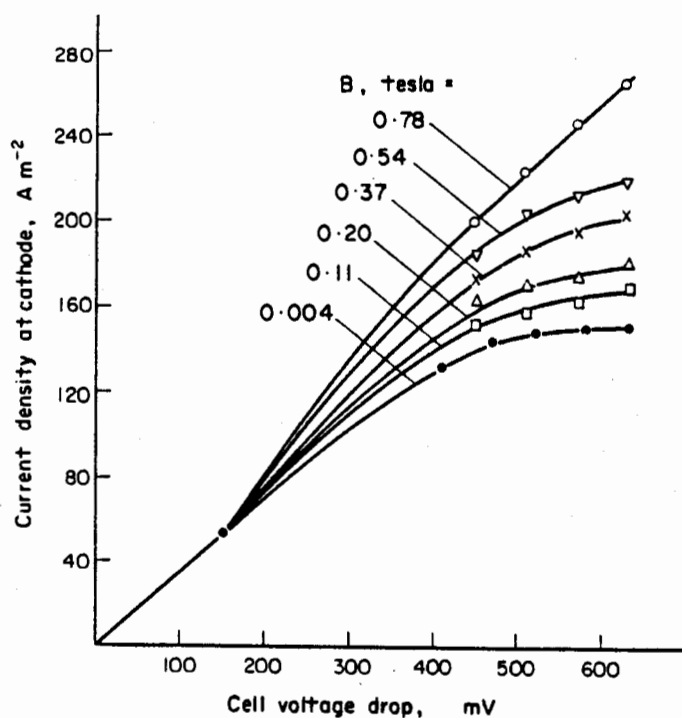
Figure 8. Typical voltage vs. time graphs for lower current density (A) and higher current density (B). Experimental conditions are shown.

Figure 8, B which is the result at 720 mA/sq cm. After 2 minutes at 420 mA/sq cm or 12 seconds at 880 mA/sq cm the cell voltage jumps over an order of magnitude from 1.5 or 2.5 volts to about 25 volts and then the voltage fluctuates violently. After the initial jump, the potential rises another 5 V or so over an interval on the order of minutes, the actual length depending upon the current density. Following this gradual increase there is a sudden drop in the low potential to roughly equal to the cell voltage before the first dramatic jump. This behavior did not repeat itself with CD's between 420 mA/sq cm and 640 mA/sq cm. For CD's of 720 mA/sq cm and above, this behavior was repeated in a manner similar to that shown in Figure 8, B.

The initial jump of the cell potential is probably the manifestation of the transition time which is the time required for the concentration of copper ions to go to zero at the cathode. Measurements of the transition time are used in finding the concentration of ions in solution in chronopotentiometry (6, p.1051). The violent voltage fluctuations might be attributed to oxygen and hydrogen gas and copper chunks being circulated around the cathode. Close observation of the anode revealed that when the voltage initially jumps, a black oxide-like layer is formed on the anode surface. This black layer summarily streams off the anode accompanied by a crackling noise and oxygen bubbles. This action results in a bright, matte anode

surface. Dash and Takeo (14) report that vortex motion of the electrolyte in the diffusion (boundary) layer for an electrolysis cell with forced electrolyte flow and applied magnetic field may "randomize the mass transfer" and alter the resistance of the solution near the electrode. The periodic potential drop and increase has yet to be understood.

Mohanta and Fahidy (8) have found that the imposition of a magnetic field during electrodeposition in a cell with mechanically pumped electrolyte has the effect of raising the limiting current. Their experiment involved the use of a flat cathode placed along the inside of a long rectangular cell through which electrolyte was forced. In addition, the cell was placed in a magnetic field. Mass transfer rates depend upon electrode and cell shape along with natural convection and bulk-flow effects, ion concentration and Reynold's number for the flow. They cite the work of Lin, Denton, Gaskill and Putnam that in general there exists a critical flow rate, in the absence of a magnetic field, where no limiting current is observed. However, they claim that for a given flow rate, ion concentration, and temperature, a critical applied magnetic flux density may exist where no limiting current is observed even at relatively moderate Reynolds numbers or flow rates. Such an example is shown in Figure 9. It is believed that the electrolyte flow aids in the



Current density-cell voltage drop relationship at various values of the magnetic flux density at medium electrolyte concentration and low Reynolds number. $c_{Cu} = 0.185\ mol\ dm^{-3}$, $c_A = 1.53\ mol\ dm^{-3}$, $T = 300.9\ K$, $Re = 4.08$.

Figure 9. Current density vs. voltage drop graph from Mohanta and Fahidy's work with a flow cell (8) showing apparent absence of a limiting current at 0.78 Tesla (7.8 kG). c_{Cu} : concentration of copper (II) ions. c_A : concentration of sulfuric acid. T : temperature. Re : Reynolds number.

transport of ions in the bulk, while the stirring arising from the applied field provides a "sweeping effect" on the electrolyte layers near the cathode. This stirring, in effect, reduces the average thickness of the diffusion layer so that the ion-concentration gradient is greater at the electrode, aiding to increase the diffusion current.

Cousins (12) reports a net decrease in the average cell voltage when both the cathode and the anode are placed in a magnetic field of 11.5 KG during electrolysis in a copper sulfate solution. He detected a voltage change of 0.265 V for just the cathode between the pole pieces, and a 0.020 V decrease in the observed cell potential with just the anode in the magnetic field. He detected between 0.200 and 0.215 V reduction in cell potential with both electrodes in the magnetic field. As can be seen, the sum of voltage change for the anode alone and the cathode alone is greater than the voltage drop when the cell (both electrodes and the electrolyte) are in the magnetic field together. This is attributed to the greater effect of the Hall magnetoresistance when both electrodes are in the cell. Although the effects of magnetically induced Hall resistance contributes to raising the cell potential when both electrodes are in the magnetic field, the net effect of an applied magnetic field is to reduce the cell potential. The overwhelming effect of the magnetic field is to increase ion transport

which reduces the concentration polarization and therefore the impedance to current flow. In addition, he states that the reduction in the cell voltage by electrolyte pumping and by magnetic field application do not work independently of one another. This means there exists a limit below which the cell potential cannot be lowered. The reason for this is that the activation overpotential must be supplied and electrolyte resistance overcome for any deposition reaction to occur. Even if a reduction in the concentration overpotential, which is caused by a build-up of ions at the anode and a depletion of ions at the cathode, occurs, an outside source of current is necessary to take the cell out of the reversible conditions.

CHAPTER IV

EFFECT ON THE UNIFORMITY OF THE DEPOSIT

An important consideration in determining the usefulness of a copper deposit is the surface morphology of the deposit. Whether it is for decorative, protective, or other uses (e.g. conductors), a smooth, uniform covering is normally desired. This usually means a deposit with a small crystalline grain size. How well a given copper plating method can cover nonuniformities such as nooks and bends is also of great interest when plating objects with holes or crevices. An example of such a use would be the plating of copper in small holes in printed circuit boards. This "throwing power" is affected by how uniformly a given process transports the metal ions to the treated surface of the electrode.

Factors affecting the uniformity

Current distribution. The current distribution is the factor which affects the distribution of metal onto the cathode. The current distribution in the absence of any polarization is called the primary distribution. The primary distribution takes into account just the ohmic resistance to current flow and is disturbed once current begins to flow. The current distribution during

deposition, when a current is flowing and polarization exists is called the secondary or actual distribution (15, p.29). Because polarization increases with current density, areas in which there is a tendency for higher current density may receive less current than expected due to higher concentration polarization. Due to such an effect, a copper deposition solution for which current efficiency drops off quickly with increased current density tends to give more uniform coverage. Thus, the sulfate bath which was used in this work is considered to have relatively poor "throwing power" in comparison to cyanide baths, for example. This is because the sulfate bath provides nearly 100% efficiency at both lower and higher current densities (16, 17, p.485).

Generally the notion that "the rich get richer, and the poor get poorer" prevails if no steps are taken to prevent protrusions from growing larger and recesses from receiving relatively less deposit. Protrusions grow larger and indentations become relatively smaller because the diffusion layer thickness will, in general, vary across the face of the electrode. As long as the cathode reaction is under diffusion control, the thickness of the diffusion layer will determine how quickly deposited material accumulates.

Surface structure effects. There exist a few ways to change the characteristics of a deposit without the

application of a magnetic field. By affecting the uniformity of the electric field at the surface of the electrode it is possible to reduce nonuniformities in the deposit. One could obtain a deposit of uniform thickness if the current density (CD) were uniform across the entire deposit surface. Thus one way to obtain a uniform deposit is to make the electric field across the surface of the electrode as uniform as possible, assuming that all sites on the electrode are equally suited for ion discharge and grain growth. In common practice, there are edge effects and macroscopic irregularities which break down the uniformity of the current distribution. In addition, the electrodes always have macroscopic defects such as scratches or bumps, and even if these can be removed by careful preparation, microscopic defects and dislocations invariably exist. Even though these defects aid in the metal deposition process (6, p.1178), these factors, nonetheless, make obtaining a uniform deposit more difficult.

Microbumps can become macrobumps visible in conventional microscopes if the conditions are favorable for their growth. The size of these microbumps, which are the result of dislocations in the metal, are initially on the order of an atomic layer. Even if the irregularities were on the order of a micron it would not be expected that the current distribution should be significantly

altered. The resistivity of the solution is sufficiently low that the electrical potential difference between the top and bottom of the microbump is negligible (15, p.32). However, because microscopic edges formed by screw and edge dislocations provide energetically convenient locations for deposition, the growth rate may be faster at these sites as long as the current density is low enough that metal atoms have time to diffuse to stable sites. Bockris and Reddy (6, p.1220) cite the work of Barton who has argued that the activation overpotential may be lower at the tip of a microspiral. A microspiral is formed when metal ions gather at the edge formed by a screw dislocation causing the edge to spiral around the dislocation as the crystal grows. Barton has also reported that the density of steps and kinks may be greater at the top of the microspiral. It is also important to mention that the substrate is multicrystalline. This means that a wide variety of different crystalline planes may be initially exposed to the electrolyte. Irregularities may arise if crystal growth occurs preferentially on certain crystallographic planes.

Addition agents. The addition of colloidal materials in small amounts can improve the smoothness of the deposit (17, p.482). The reason given for this is that the colloids become adsorbed onto the crystal nuclei

preventing their growth. In addition to preventing growth, these colloids aid in nuclei production by providing heterogeneous nucleation sites. These colloids are usually organic substances such as molasses, albumin or cellulose fibres. Through their action very small grained deposits can be produced.

Solution resistivity and throwing power. The copper sulfate solution which was used in this study is generally believed to be a plating solution with poor macro-throwing power (15, p.30). The macro-throwing power is the measure of how well a given plating system produces a uniform coverage over an electrode with macroscopic irregularities. In general the throwing power of a copper deposition electrolyte is thought to be better if the solution has a relatively high resistivity. That means that the slope of the voltage versus current density graph will be steep (17, p.485). In other words, a small increase in the local potential will not cause a significant increase in the local effective current density. In a solution with low resistivity, such as the copper sulfate solution, a small change in the local electric field may significantly affect the local current density. With a low resistance solution, it is clear that if the current density is higher more ion discharge and consequently more deposition occurs so long as the limiting current is not locally exceeded. Given a

solution with high resistivity, it would be expected that small macroscopic protrusions or indentations will not significantly affect the local electric field, and coverage will tend to be evened out. Furthermore, if the conductivity of a solution is significantly improved, the macroscopic throwing power should be decreased for the same kind of reasoning.

RESULTS AND DISCUSSION

The deposits shown in Figures 10 and 11 show a smoothing of the deposit as the magnetic field is increased. Photo B, Figure 11 shows the effect on the deposit of doubling the current density from the deposit in photo A of the same figure. Generally, increasing the current density while maintaining the other parameters constant is expected to give a finer grained deposit (18). A finer grained deposit is favored at higher current densities because the metal atoms are arriving on the electrode surface so quickly that they have no time to surface diffuse to positions which would maintain previous growth patterns (15, p.9).

The dendritic deposit shown in Figure 10, A, indicates that the limiting current was exceeded. In such a case the formation of dendrites is favored because of the depletion of copper ions near the electrode. As Bockris and Reddy (6, pp.1218-1219) write,

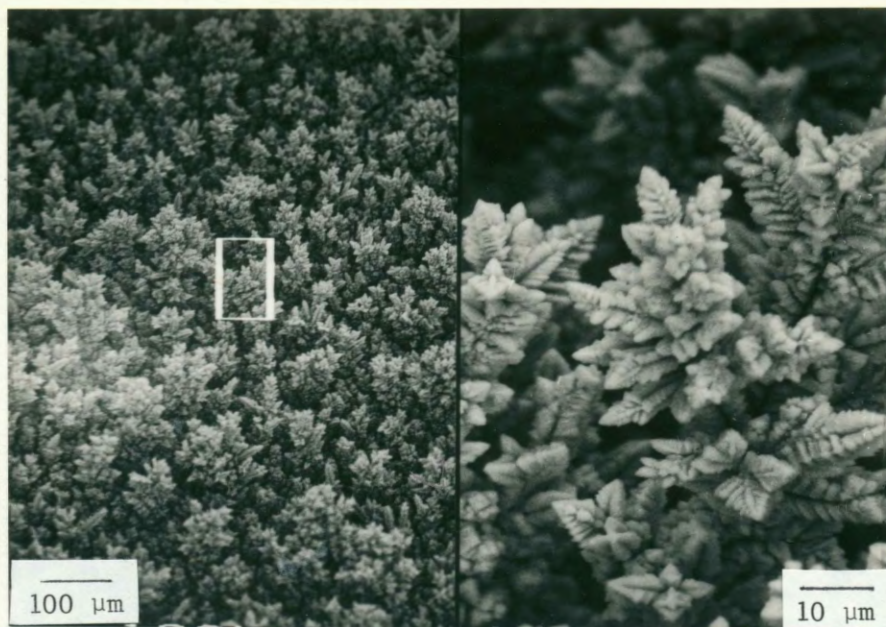


Photo A

CD =
80.0 mA/cm²

B = 0.11 kG

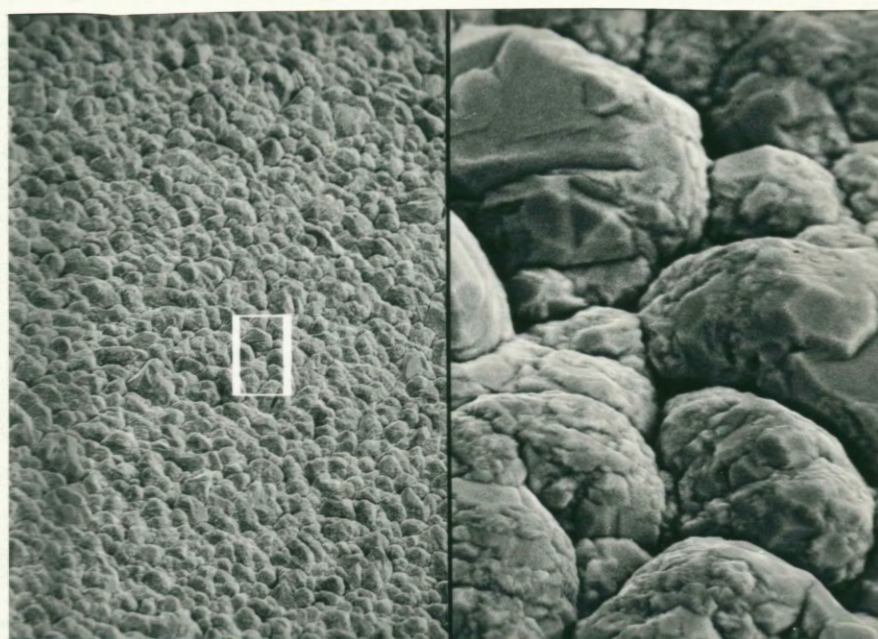


Photo B

CD =
80.0 mA/cm²

B = 1.55 kG

Figure 10. SEM micrographs of the morphology of copper deposits produced from anodes shown in Figure 17. The magnetic field and current densities are as shown. The magnification markers shown in Photo A apply to both photographs. Photo A shows a powdery dendritic deposit. Photo B shows a compact deposit. Both deposits were produced in the smaller diameter cell without a water jacket.

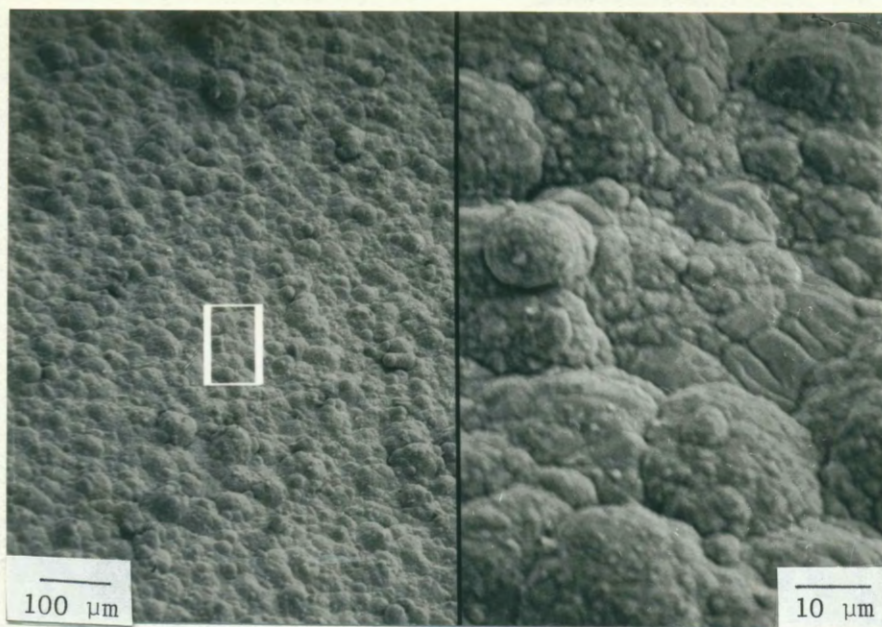


Photo A

CD =
80.0 mA/cm²

B = 10 kG

Run 42

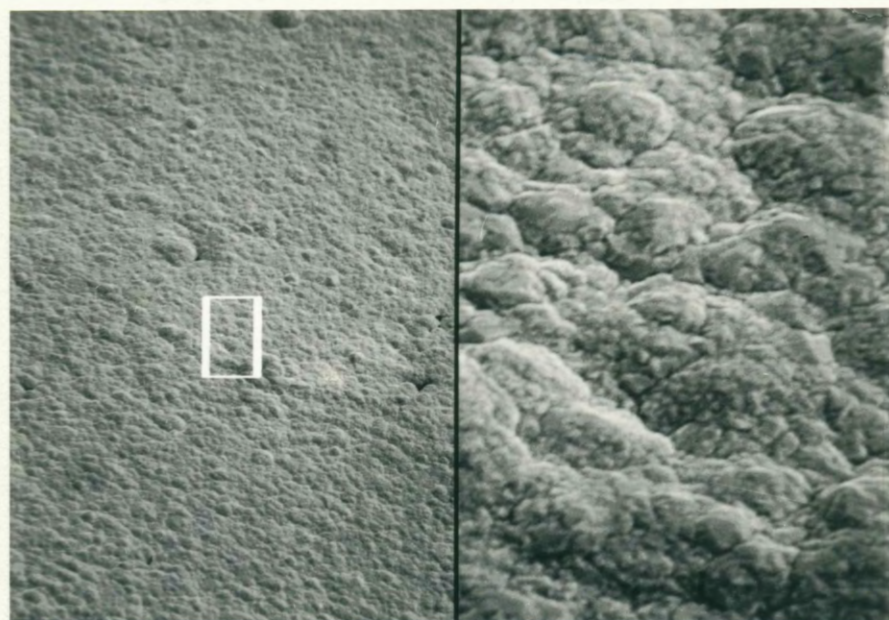


Photo B

CD =
160 mA/cm²

B = 10 kG

Run 57

Figure 11. SEM micrographs of the morphology of copper deposits produced from anodes shown in Figure 18. The magnetic field and current densities are as shown. The magnification markers shown in Photo A apply to both photographs. Both deposits were produced in the smaller diameter cell without a water jacket. Photo A shows a compact deposit, and Photo B shows a compact deposit produced at the same magnetic field as in Photo A but at twice the current density.

The nature of the further growth depends on how easily different parts of the electrode secure the supply of ions used to build up the crystal surface. One is talking of the logistical differences between different parts of the advancing crystal front.

Through the formation of such dendrites the deposit surface "seeks out" regions of higher ion concentration in the bulk solution. Furthermore, if the electrode reaction is under diffusion control, which is the case at high concentration overpotentials, the limiting current at the tip of the dendrite is thought to be greater than the surrounding regions (9, p.200). The reason for this is that as the radius of curvature of the substrate, r , becomes much smaller than the diffusion layer thickness, δ , the limiting current varies as $1/r$ instead of $1/\delta$. Thus, the limiting current is,

$$i_{\text{limit}} = \frac{n D F c}{r} \quad \text{for } r \ll \delta.$$

Where n is the number of electrons necessary for one reaction to occur, D is the diffusion constant, F is Faraday's constant (96500 C), c is the bulk concentration of metal ion in the solution, and r is radius of curvature of the tip.

According to Drazic (9, p.200) these dendrites start to grow when a spiral formed by a screw dislocation grows above the surrounding electrode region, so that the diffusion layer is thinner at the tip of the dendrite than

on the flat part of the electrode. He mentions that a critical potential is necessary for the growth of the spiral.

Some representative higher current density deposits are shown in Figures 12 and 13. The deposit in photo A, Figure 12 is still compact and well-adherent. Photo B, Figure 12 shows some "worm holes" which probably are produced when hydrogen bubbles stick onto the deposit surface preventing deposition. Also the deposit has changed to the round nodules characteristic of rough deposits where hardness measurements cannot be performed. In Figure 13, at 880 mA/sq cm CD the surface is quite rough and powdery. There also appears a dendrite which seems to be growing out from the surface of a nodule. It is possible at such high CD and concentration polarization that the diffusion layer at this nodule was sufficiently thin to favor dendritic growth.

Deposition onto TEM grids. In our attempts to study the effect of a magnetic field on the deposit coverage uniformity, we not only used the aforementioned square cathodes, but copper deposited onto grids used to hold transmission electron microscope (TEM) specimens were also studied. These specimen grids are made up of two 3 mm copper circles with a hinge section as shown in Figure 14, A. The full view of grids with deposits is also shown in Figure 14, B-E. The basic equipment used in depositing on

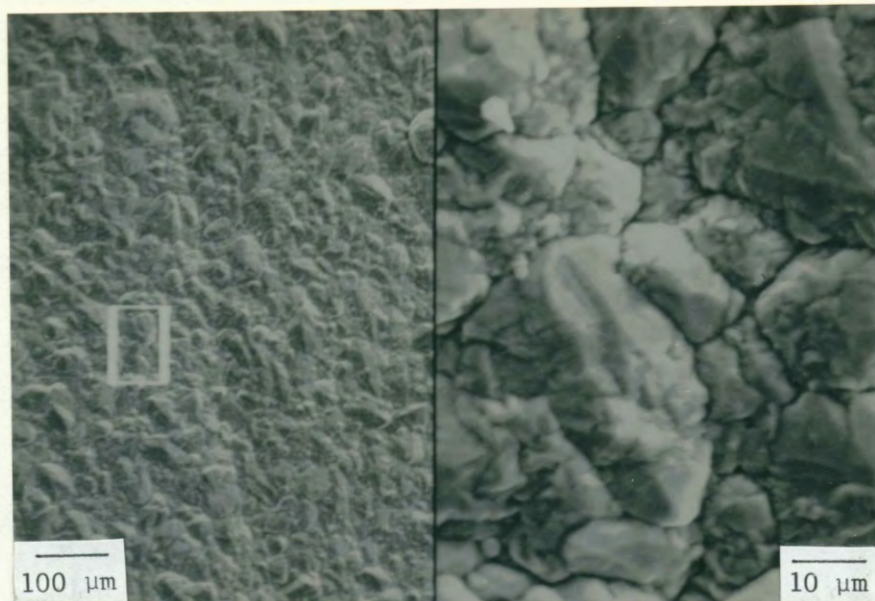


Photo A

CD =
190 mA/cm²

Run 78

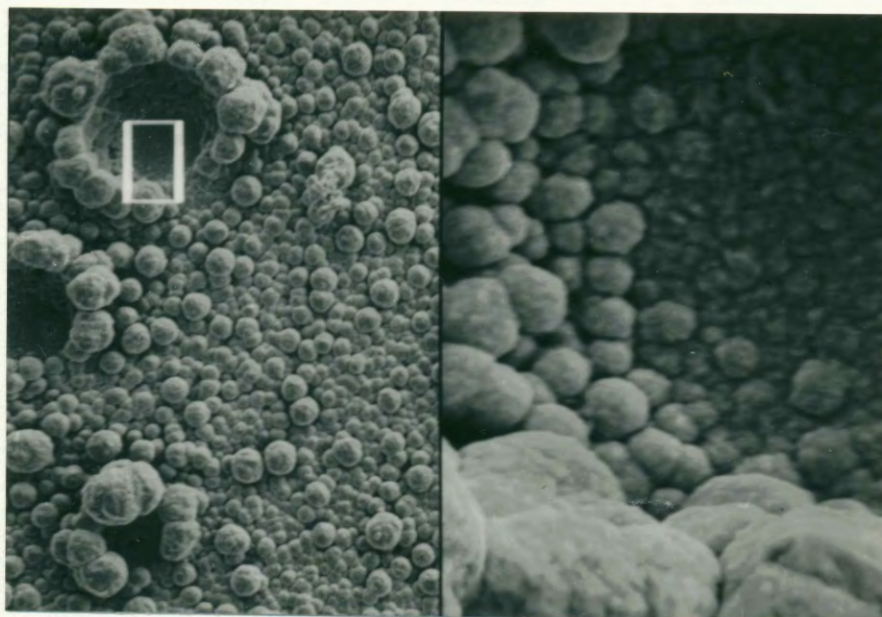


Photo B

CD =
360 mA/cm²

Run 115

Figure 12. SEM micrographs of the morphology of copper deposits produced from the anodes shown in Figure 19. The magnetic field was 7.40 kG for each run, and the current densities are as shown. Magnification markers in Photo A apply to both photographs. Photo A shows a compact deposit. Photo B shows a non-compact deposit with "worm-holes" produced when copper grows around gas bubbles on the surface of the cathode.

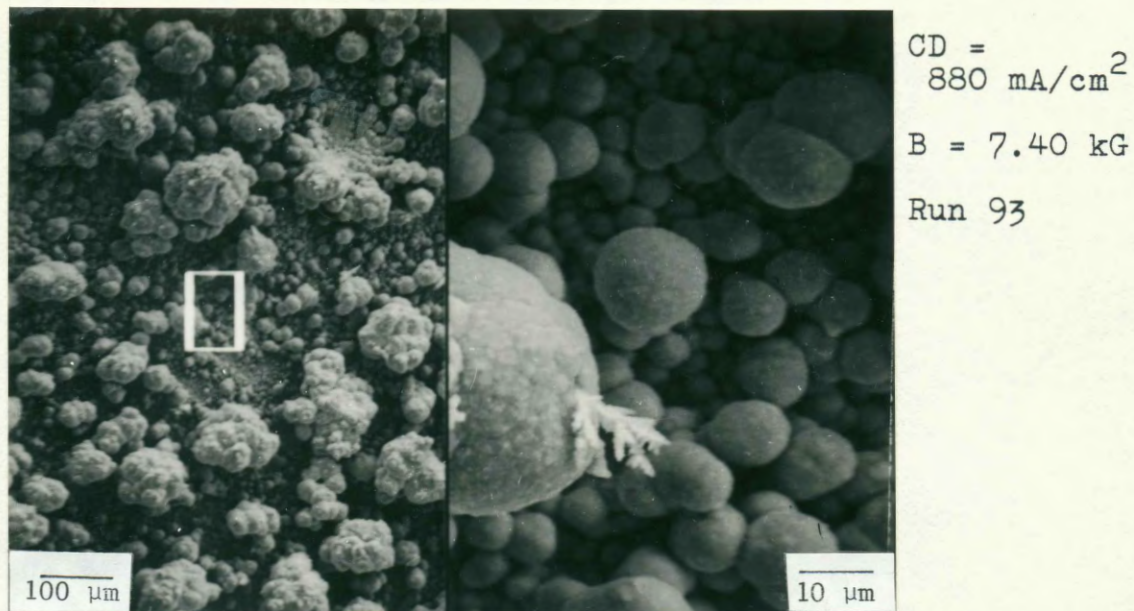


Figure 13. SEM micrograph of the morphology of copper deposit produced from the anode shown in Figure 20, B. The magnetic field, current density and magnification are as shown. Deposit was produced in the larger diameter water-jacketed cell. This photo shows a non-compact deposit with a dendrite appearing to be growing out of a nodule.

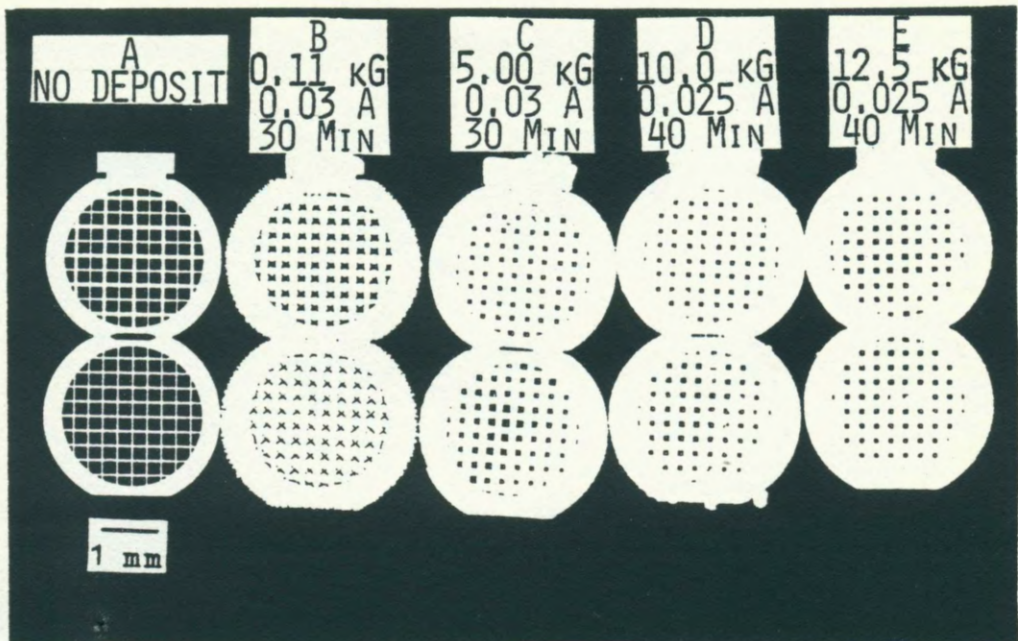


Figure 14. Full view of copper grids showing the effect of a magnetic field on copper deposition into small holes. All surfaces were parallel to the magnetic field except upper surface of grid D which was oriented perpendicular to the field. Exposed area of the grid is $0.155 \pm .005 \text{ cm}^2$. Magnification marker applies to all photographs. Current, deposition time are shown along with applied magnetic field.

the TEM grids was the same as in the other experiments. The current densities also were kept in the same range (between 100 and 200 mA/sq cm). By observing how the holes in the grid had retained their original shape one determined the uniformity of the deposit.

Through-hole plating involves depositing metal into a small hole as in the TEM grids or printed circuit (pc) boards. In pc boards such deposits serve as connectors between conductors on opposite sides of the board. Copper is chosen because of its solderability, good corrosion characteristics and mechanical properties (16).

In the case of the TEM grids the effect of a magnetic field is readily apparent upon study of Figure 15. The deposit produced at 0.11 kG (residual field) appears to have non-uniform coverage of the grid hole. The deposit grows in from the sides of the hole leaving the corners with little or no deposit which produces a "pin cushion"-like deposit. As the magnetic field is increased there is improved retention of the original, square-hole shape, so that at 10 and 12.5 kG the deposit contains holes with the same shape as before depositing. The hole size is, of course, smaller because of the significant amount of copper deposited into the hole.

The "pin-cushions" are formed when only the residual field is applied and they gradually disappear at higher magnetic fields. Without any applied magnetic field, the

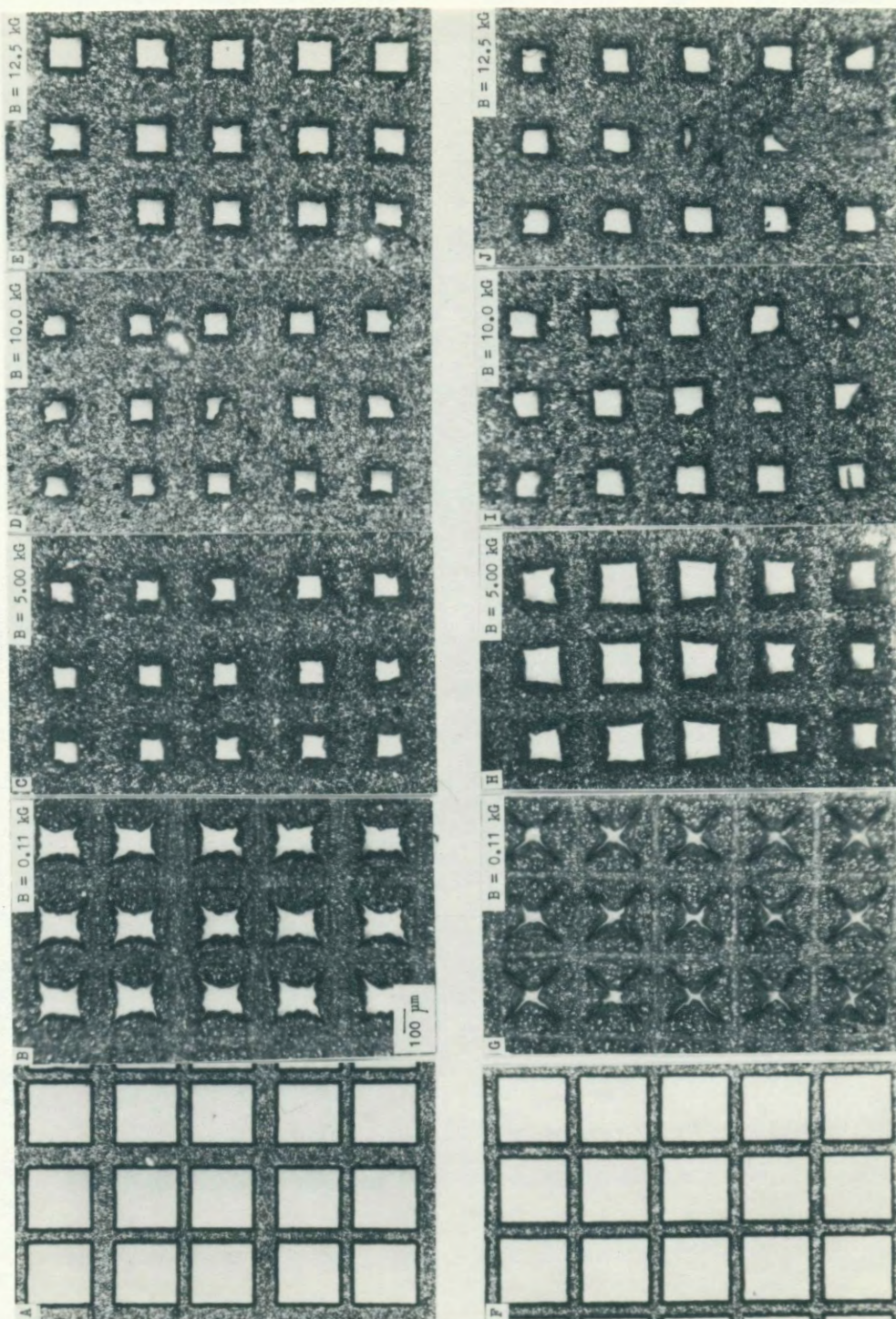


Figure 15. Magnified view of copper grids showing the effect of a magnetic field on deposition into small holes. All surfaces parallel to magnetic field except as noted. A, F: upper (A) and lower (F) surfaces of a grid before depositing copper. B, G: B = 0.11 kG. C, H: B = 5.00 kG. D, I: B = 10.0 kG with upper surface (D) perpendicular to field. E, J: B = 12.5 kG. Magnification marker in B applies to all photographs.

corners of the holes receive the smallest current density of copper ions as can be detected from the lack of deposit there. Most of the electric field lines are likely to be concentrated at the sides of the holes. This is because two like charges on adjacent sides of the square hole will tend to repel one another thus avoiding the areas near the corners. Also, there is competition for copper ions between the two adjacent sides of a hole which meet at a corner. Because of this type of competition, one would expect a thicker diffusion layer at the corners (19). On the other hand when a magnetic field is applied, the Lorentz force which aids in the stirring also causes the ions to be deflected from the path along electric field lines. In addition, wherever the current distribution has a tendency to be the strongest, there will be a greater number of ions, and therefore the effect of this magnetoresistance on the transport of ions will be greater. Thus, along the sides of the holes where the electric field has a tendency to be stronger the effect of the "magnetoresistance" is greater, and the uniformity of the deposit in the hole is improved.

Another effect of the applied magnetic field may arise from the stirring which occurs. As the transport of ions through the bulk solution is improved the uniformity of the ion concentration at the electrode improves the uniformity of the deposit and also reduces the

concentration overpotential. Through agitation, the diffusion layer thickness inside the hole may be altered so that a greater flux of copper ions arrives at the corner of the hole helping to produce a more uniform coverage inside the hole.

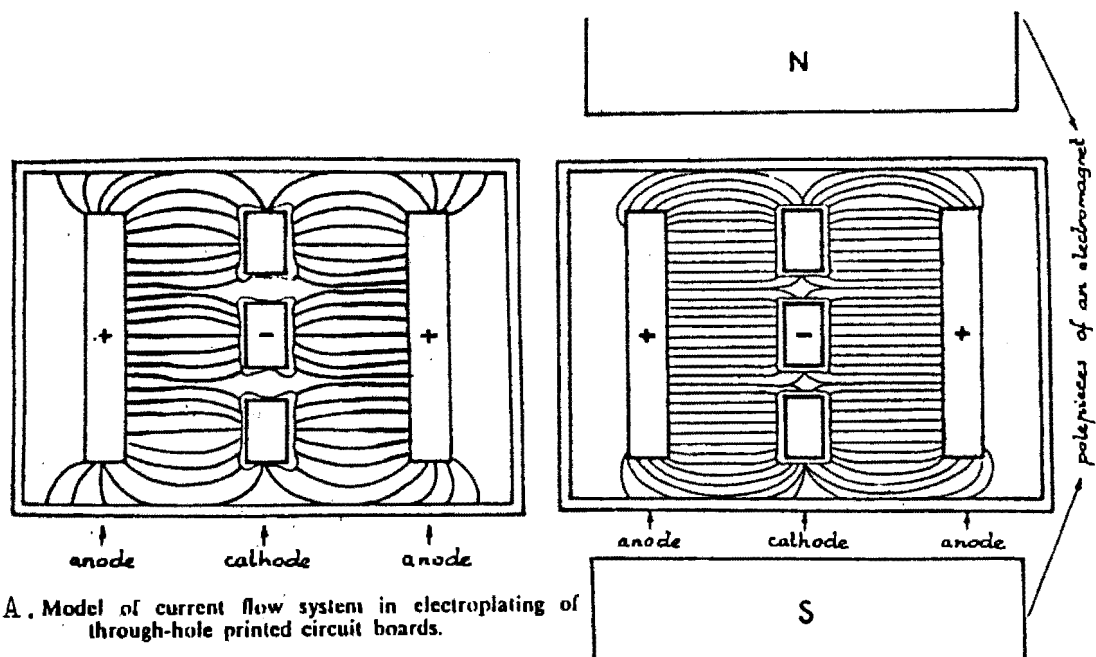
FINDINGS OF OTHER WORKERS

Dash, along with King (20), as well as Csokan (21) have found that the application of a magnetic field during through-hole plating greatly improves the uniformity of the deposit in the hole.

Wildwood (22) suggests that the magnetic field may affect the behavior of the electrons in the electrode which are available to tunnel to the charged ion in order to discharge it. He claims that the likelihood of these electrons being in singly occupied orbitals is great, so they are paramagnetic and would tend to line their magnetic moments along the magnetic field lines. He notes that the electrons which are in position to tunnel to the ion to discharge it must be near the surface of the electrode. Since the magnetic fields which were applied in his experiments were uniform, these tunnelling electrons, being paramagnetic, would have a tendency to line up their magnetic moments with the magnetic field. distribute themselves more uniformly in the conductive electrode and so the deposits were more uniform.

Csonkan (21) displays how the electric field might be distributed before and after the magnetic field is applied (Figure 16). Without the application of a magnetic field the electric field lines are concentrated on the edges of the holes on the electrode. He contends that with the application of a magnetic field, the electric field lines become uniformly spaced giving a more uniform current distribution and consequently a more uniform deposit coverage. He also mentions the Hall-effect-like magnetoresistance.

The migration path of ions between two collisions may be deflected intermittently from the direction of the magnetic field orientation (zigzag or spiral path) in which case voltage differences will occur in the solution, similarly to the Hall effect with solid conductors. The electromagnetic alternating effects mentioned explain how the current distribution, that is the throwing power of the electrodeposition, on the cathode surface can be influenced by superimposed magnetic forces affecting the cell voltage such that the ion migration paths can penetrate even depressions and narrow recesses of the surface.



A. Model of current flow system in electroplating of through-hole printed circuit boards.

B. Model of current flow system in electroplating of a through-hole printed circuit board using superimposed magnetic field.

A

B

Figure 16. Effect of applied magnetic field on current distribution from Csonkan (21). A shows the current distribution which results in poor uniformity inside the holes. B shows the current distribution after a magnetic field is applied resulting in a more uniform deposit.

CHAPTER V

SURFACE MORPHOLOGY OF THE ANODES

In addition to looking at the cathode, we also studied the anode surface appearance. Electrolytic thinning is one method of obtaining a sufficiently thin (electron-transparent) transmission electron microscope specimen. Chemical thinning and polishing is another method. Unfortunately, with both methods poor overall uniformity and preferential thinning at the edges of the specimen often doom even the most hopeful attempts at obtaining a suitable sample. Also, electrolytic polishing is one method of obtaining a shiny finish while being able to carefully control the rate and extent of thinning. Since each time a cathode is produced, an anode is also produced, it seemed only prudent to look at its surface morphology also.

The anodes were made of the same material and produced in the same fashion as the cathodes except that during the experimental run both sides of the anode were exposed to the copper sulfate solution.

Scanning electron micrographs clearly show the surface structure of the anodes. Figure 17 shows two anodes both thinned at 80 mA/sq cm. The anode at 0.11 kG has an etched surface, but the anode at 1.55 kG is

smoother.

The anode in Figure 18, A, shows a dramatic etching effect with dissolution taking on a step-like appearance. Incidentally, the cell voltage was lowest at 10 kG for the set of runs at 80 mA/sq cm from which these anodes were taken. The etching type of anode dissolution takes place when it is energetically preferred for dissolution to take place along certain "weaker" regions such as grain boundaries and dislocations. The step-like dissolution pattern looks similar to crystal electrogrowth (6, p.1204-1217) along steps and kinks on the cathode.

Various degrees of etching between Figure 17, B, and Figure 18, A, are observed for the anodes between 1.55 kG and 10 kG. At 80.0 mA/sq cm current density no smooth anodes were produced. However at the higher current densities (CD) anodes with smooth surfaces are seen.

Photo B in Figure 18 shows the anode at 160 mA/sq cm and 10 kG. It is relatively smoother but yet is dull to the naked eye. Anodes produced at higher current densities are shown in Figure 19 and 20. At 190 mA/sq cm (Fig. 19, A), the surface becomes more roughly etched, and the "gouged out" appearance again prevails. At 360 mA/sq cm (Fig. 19, B) the surface becomes quite uniformly smooth. In the magnified view to the right, the surface shows many small holes (etch pits) which give the anode a matte finish. At 560 mA/sq cm (Fig. 20, A) a similar kind

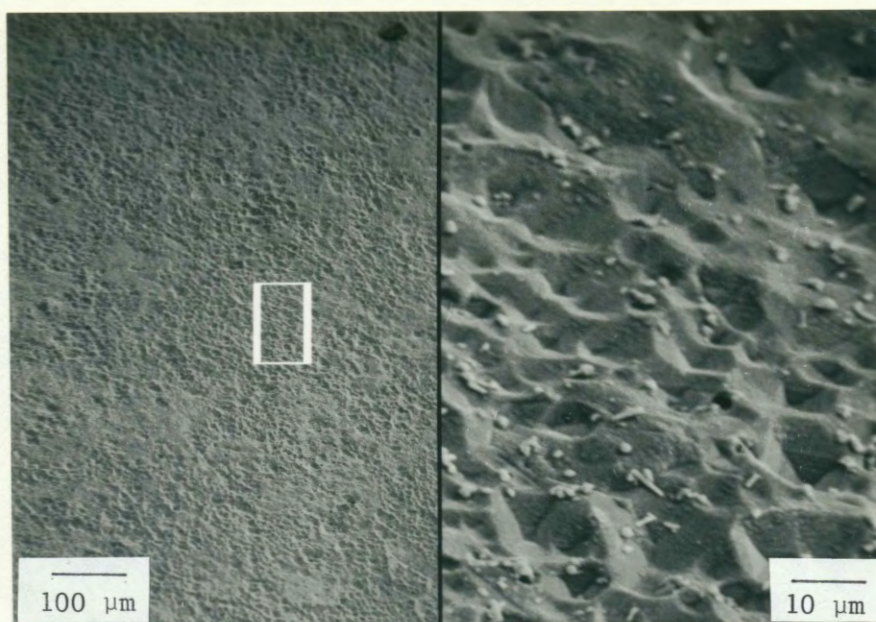


Photo A

CD =
80.0 mA/cm²

B = 0.11 kG

Run 30



Photo B

CD =
80.0 mA/cm²

B = 1.55 kG

Run 47

Figure 17. SEM photomicrographs of the morphology of copper anodes used to produce deposits shown in Figure 10. The magnetic field and current densities are as shown. The smaller diameter cell without the water jacket was used. The magnification markers in Photo A apply to both photographs.

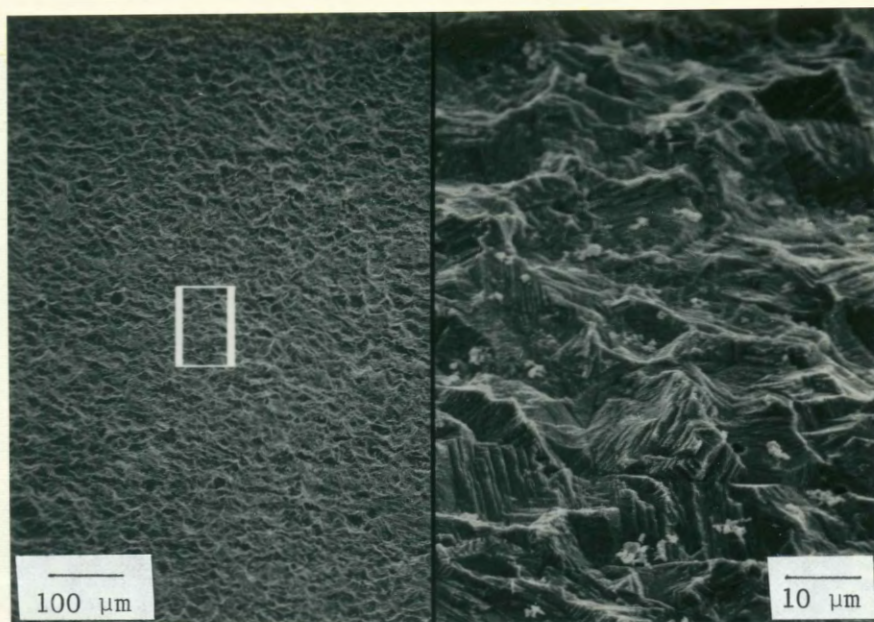


Photo A

CD =
80.0 mA/cm²

B = 10.0 kG

Run 42

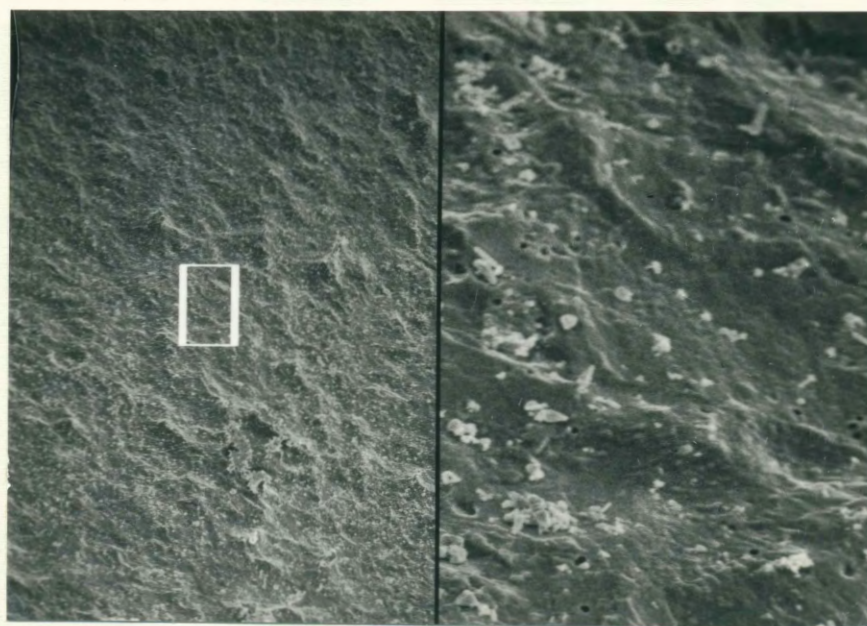


Photo B

CD =
160 mA/cm²

B = 10.0 kG

Run 57

Figure 18. SEM photomicrographs of the morphology of copper anodes used to produce deposits shown in Figure 11. The magnetic field and current densities are as shown. The smaller diameter cell without the water jacket was used. The magnification markers in Photo A apply to both photographs.

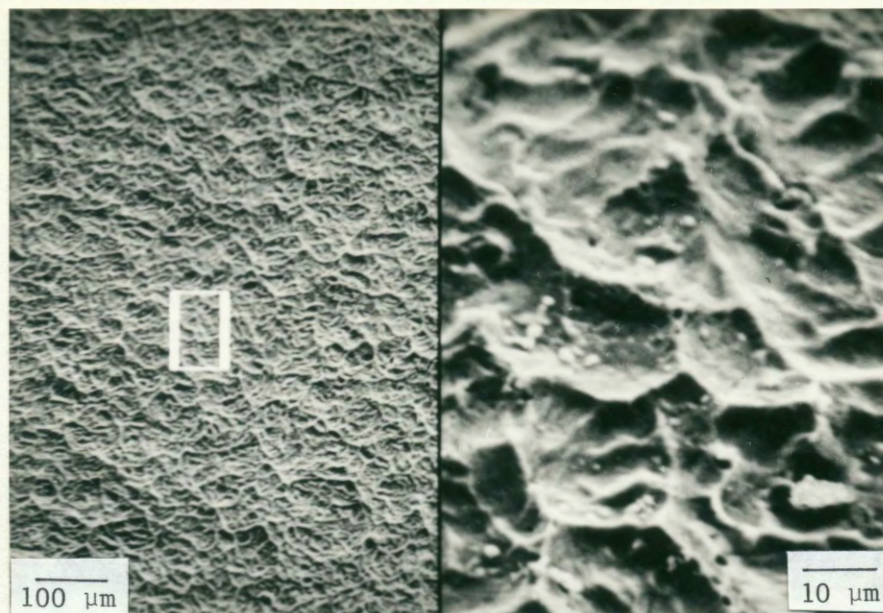


PHOTO A

CD =
190 mA/cm²

B = 7.40 kG

Run 78

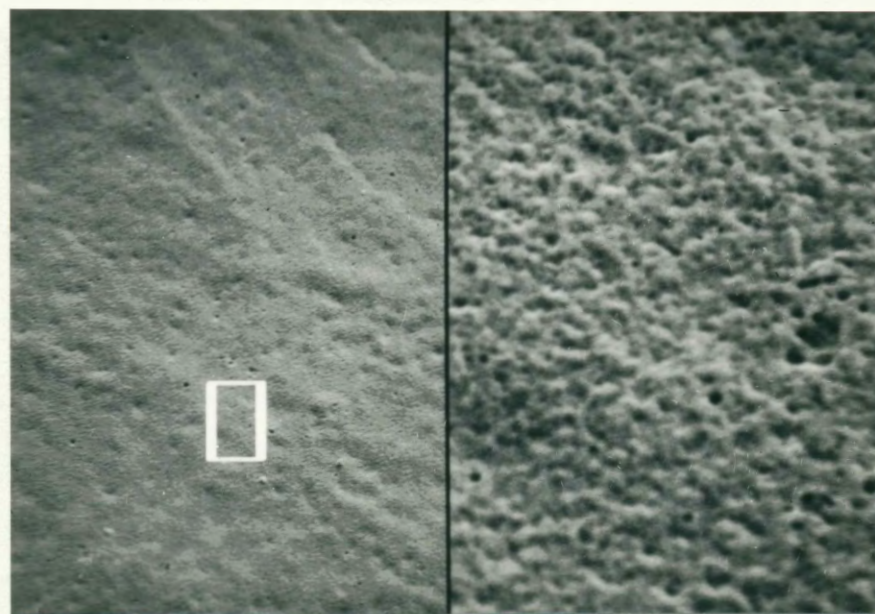


PHOTO B

CD =
360 mA/cm²

B = 7.40 kG

Run 115

Figure 19. SEM photomicrographs of the morphology of copper anodes used to produce deposits shown in Figure 12. The magnetic field, $B = 7.40$ kG for each run. The water-jacketed cell was used, and the current densities are as shown. Magnification markers in Photo A apply to both photographs.

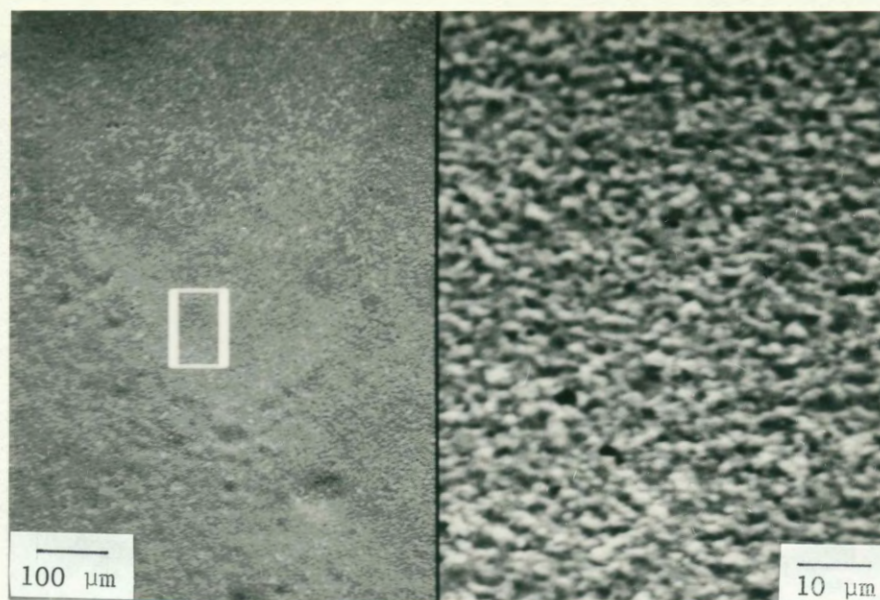


Photo A

 $CD = 560 \text{ mA/cm}^2$ $B = 7.40 \text{ kG}$

Run 107

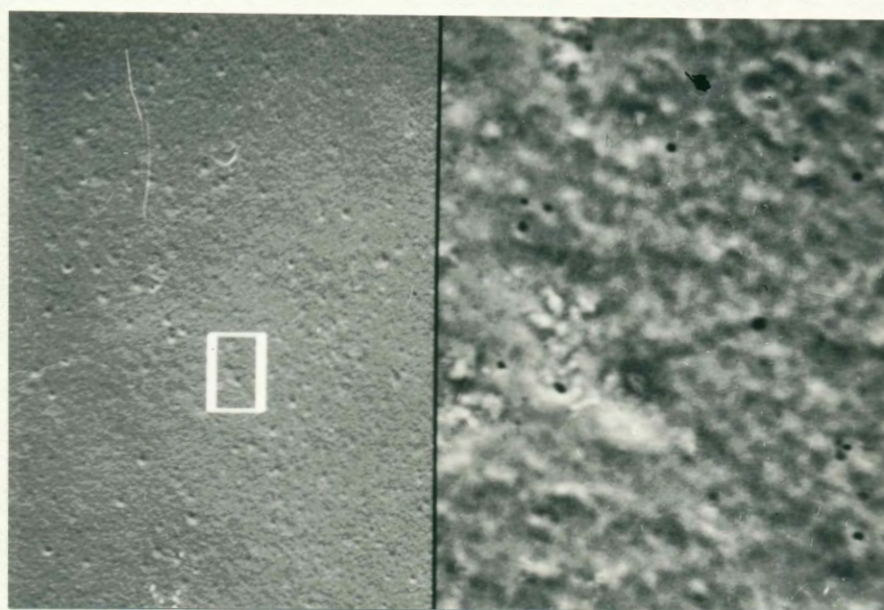


Photo B

 $CD = 880 \text{ mA/cm}^2$ $B = 7.40 \text{ kG}$

Run 93

Figure 20. SEM photomicrographs of the morphology of copper anodes. Cathode for Run 93 is shown in Figure 13. The magnetic field and the current densities are as shown. The water-jacketed cell was used. Magnification markers shown in Photo A apply to both photographs.

of surface is observed. At 880 mA/sq cm (Fig. 20, B) the surface has few etch pits and takes on a uniformly bright and matte appearance. The bright white specks on the anodes are believed to be oxides which tend to be insulating and therefore charge up with electrons in the SEM.

DISCUSSION

A typical current versus voltage curve for the anode would look like that shown in Figure 21 (23, p.3). This I vs. V curve was found by Tegart for the orthophosphoric copper thinning solution originally used by Jacquet. In the caption for the graph are shown the surface characteristics for the regions shown. In thinning there are two processes necessary to obtain a smooth and bright surface. Smoothing involves the elimination of large-scale irregularities, and brightening involves the removal of the smaller ($>1/100$ micron) irregularities. The formation of a relatively thick viscous layer of reaction products around the anode controls the smoothing action. The formation of a thin film on the surface of the anode controls the brightening action (23, p.2).

In considering our results, we believe that the etched anodes were obtained at conditions comparable to the A-B range. In this region the current density is low enough that the operative transport processes keep the

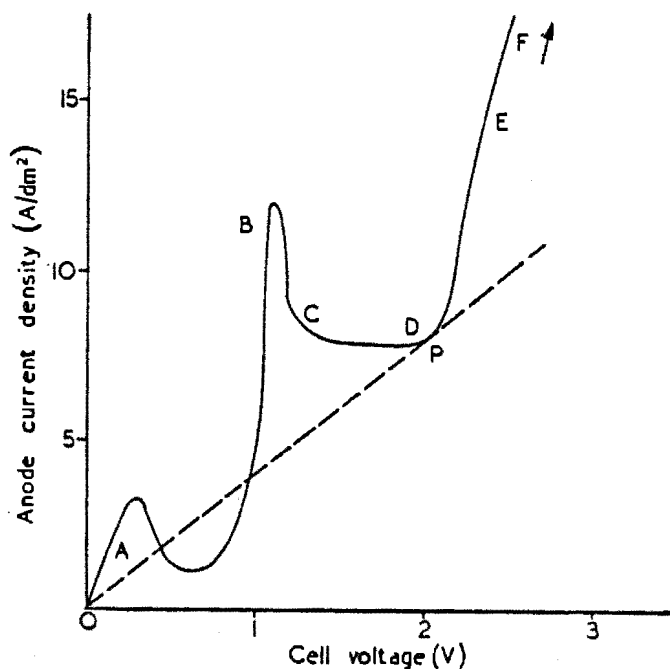


Figure 21. Cell voltage as a function of anode current density for copper in 900 g/l orthophosphoric acid. The regions on the cell voltage curve can be distinguished as: A-B etching; B-C unstable; C-D stable plateau with polishing; D-E slow gas evolution with pitting; E-F polishing with rapid gas evolution. P indicates optimum polishing conditions. From Tegart (23).

concentration overpotential fairly low. Thus the increase in the concentration of copper ions near the electrode can be maintained at a relatively low level. This means that the thickness of the viscous boundary layer is mostly constant around the entire anode. In this case all regions would be equally likely to dissolve unless there are regions which intrinsically tend to dissolve more readily. When etching occurs such a condition is manifested.

When the current density is increased the concentration polarization increases, and the concentration of Cu(II) ions near the anode is significantly greater than in the bulk. When this condition prevails the thinning process is under diffusion control and regions from which dissolved ions can be most expediently removed dissolve most quickly. Thus protrusions are the first to be removed, and a smooth anode results. When pitting is seen we might be in a D-E type region.

Tegart (23, p.5) cites the findings of Hickling, Higgins and others in noting that the polishing process is diffusion-controlled. In the region C-D the anode is covered with a viscous layer which Jacquet found "relatively thick compared to the surface irregularities, and that there is an approximately plane interface between the layer and the bulk of the solution." He also notes

that Walton showed that polishing is intimately connected to this viscous layer. Since no truly polished anodes were found with our copper sulfate-sulfuric acid solution, it is possible that this solution is unsuitable for viscous layer formation and polishing.

Tegart summarizes his work as well as that of Vines, Hoar and Mowat (23, p.13).

The existence of a thin surface film during polishing provides an explanation for the difference between etching and brightening conditions. If the electrolyte has free access to the surface of the anode, etching results, because dissolution of the metal occurs preferentially from sites of high energy. In order to obtain a bright surface such preferential attack must be prevented. Although the exact role of the surface film in brightening is uncertain, a possible explanation can be suggested. The film follows the contours of the surface and is attacked uniformly by the electrolyte. Thus, in order to maintain the film, the passage of metal ions across the metal/film interface occurs at the same rate at all points. This causes brightening, for, as Edwards has shown, such uniform removal of metal from a surface will remove irregularities.

The application of a magnetic field just to the anode is effective in reducing the total cell concentration overpotential only to a small degree (about 10% as effective as putting both electrodes in the field) as Cousins (12) has shown. Altering the transport of ions away from the anode affects the concentration of the copper ions next to the anode, thereby affecting the anodic film which controls the dissolution characteristics of the surface. Since the anodic boundary layer and film

are important factors in obtaining a desired polish, and good polishing tends to occur at fairly high cell potentials (23, p.3), it is unclear whether magnetic field application is necessarily a favorable condition in producing a bright surface. However, electrolysis in a magnetic field is perhaps likely to produce more equal thinning across the entire anode preventing specific edge attack. The reason for this is similar to that found at the cathode. If the electric field is larger in a particular region the effect of the magnetoresistance is likely to be greater in such a region. Since the just released metal ions cannot move readily away from the anode surface, the dissolution process is inhibited. Although no conclusive results have been obtained, there is some evidence from work in this lab that such an even-thinning effect might be seen in chemical thinning (24).

CHAPTER VI

MECHANICAL PROPERTIES: HARDNESS

The Knoop hardness for the deposits was found as stated in the chapter on experimental procedure. The Knoop hardness was chosen as a representation of the mechanical properties of the deposits.

One item of interest pointed out by Vagramyan and Solov'eva (25) is that the hardness of electrodeposits can always exceed the hardness of metals obtained by other methods such as smelting without additional working or treatment. This is because it is possible to produce deposits with very small grains and a variety of structures either through the use of various additives to the electrolyte, or as in this case through the application of a magnetic field.

RESULTS

The grain structure tends to mimic the substrate structure especially near the interface between substrate and deposit. Initially this is true for all deposits (18). In the case of epitaxial growth, the grains from the substrate continue to grow straight across the interface into the deposit. Where epitaxial growth is favored the hardness of the deposit should be similar to

the substrate. Such an example can be seen in Figure 22 photos D and F. In photo D, which is a deposit at 10 kG and 80 mA/sq cm, deposit hardness is 83 KHN and substrate hardness is 80 KHN. In photo F, a good example of epitaxial growth is seen in the lower right hand corner of the picture, with the substrate hardness of 79 KHN and the deposit hardness of 89 KHN.

Tables IV and V show hardness data plotted in Figures 23-26 as a function of the applied magnetic flux density for 80 mA/sq cm current density, except as noted. Figures 23 and 25 show data for the surface perpendicular to the magnetic field. Figures 24 and 26 show data for the surface parallel to the magnetic field (See Figure 6 on hardness mounting). For the deposit hardnesses plotted in Figures 23 and 24, the substrate hardness was in the range from 80 to 90 KHN as is shown in Table IV along with the other pertinent data. For Figures 25 and 26 the substrate hardness was in the range 50 to 60 KHN. Consequently the deposit hardnesses tend to be greater for the former set of deposits. It must also be noted that the former results were obtained from deposits produced in the small diameter cell so that a higher magnetic field could be produced. Both sets of data show what seems to be a cyclical effect. That is, the hardness increases then decreases. It is necessary to do further work in the higher magnetic field range before any conclusions can be

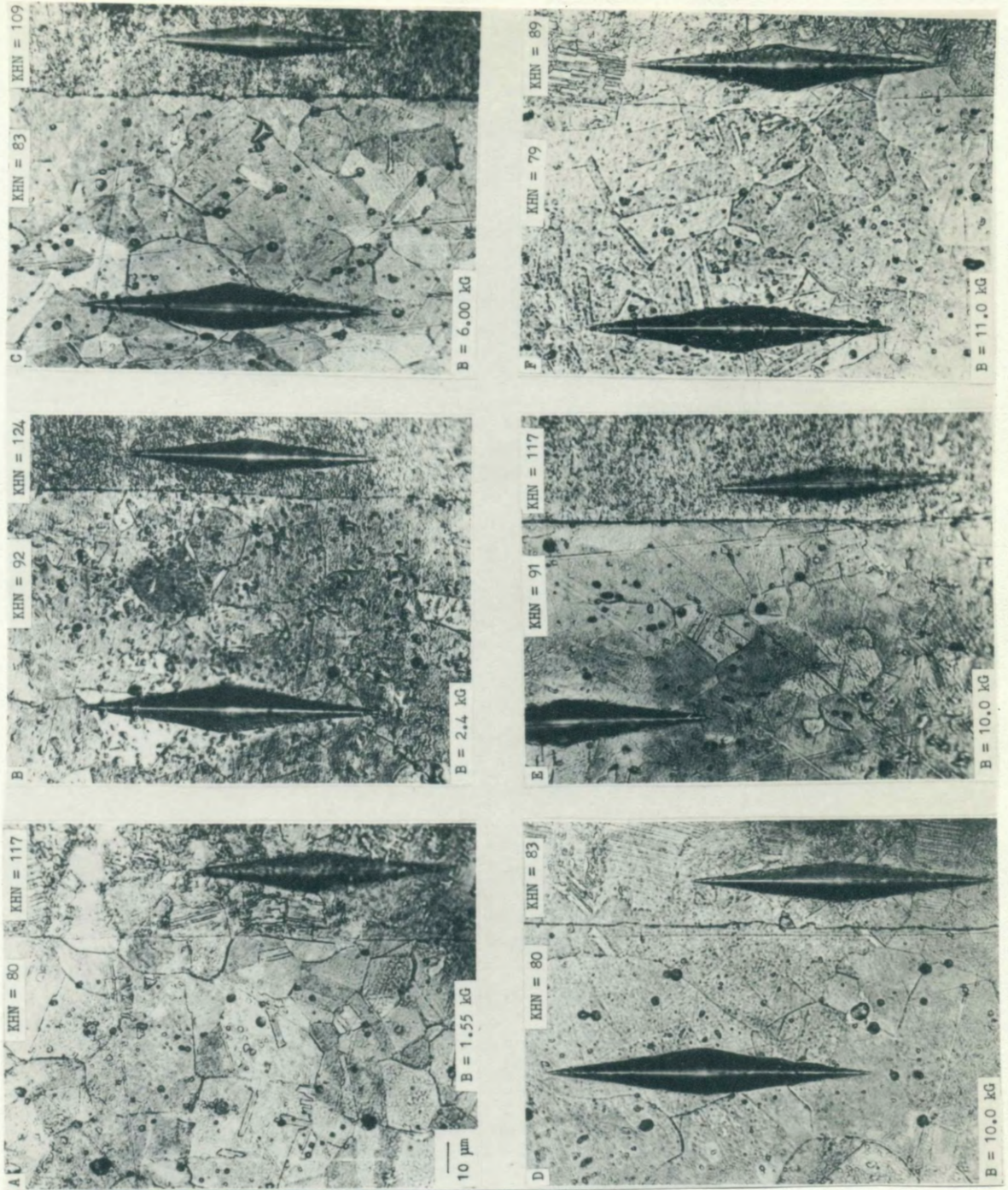


Figure 22.
 Polished and
 etched cross
 section
 surface
 showing Knoop
 hardness
 indentations
 made with a
 50 gm load.
 Current
 density =
 80 mA/cm²,
 except E,²
 160 mA/cm².
 Magnification
 marker in A
 applies to
 all
 photographs.

TABLE IV

HARDNESS OF DEPOSITS AND SUBSTRATE
 SMALLER DIAMETER CELL W/O TEMPERATURE CONTROL
 SUBSTRATE HARDNESS MISSING FOR PERPENDICULAR ORIENTATION
 FIVE INDENTATIONS EACH, WITH A 50 GM LOAD

RUN #	B KG	CD mA/sq cm	ORIENT*	DEPOSIT KHN			SUBSTRATE KHN		
				AVG	LO	HI	AVG	LO	HI
47	1.55	80.0		117	105	127	80	74	89
			⊥	72	51	95			
34	2.40	80.0		124	114	139	92	81	101
			⊥	107	90	118			
40	5.80	80.0		109	81	143	83	79	88
			⊥	89	69	130			
45	7.50	80.0		91	86	96	78	71	85
			⊥	71	65	83			
44	9.20	80.0		62	44	70	80	72	91
			⊥	77	48	133			
42	10.0	80.0		83	73	98	80	73	94
			⊥	86	54	122			
57	10.0	160		117	96	129	91	86	102
			⊥	107	66	131			
28	11.0	80.0		89	80	102	79	64	94
			⊥	86	72	124			
36	12.5	80.0		95	87	104	83	80	87
			⊥	110	97	131			

*See Figure 6, Chptr. 2.

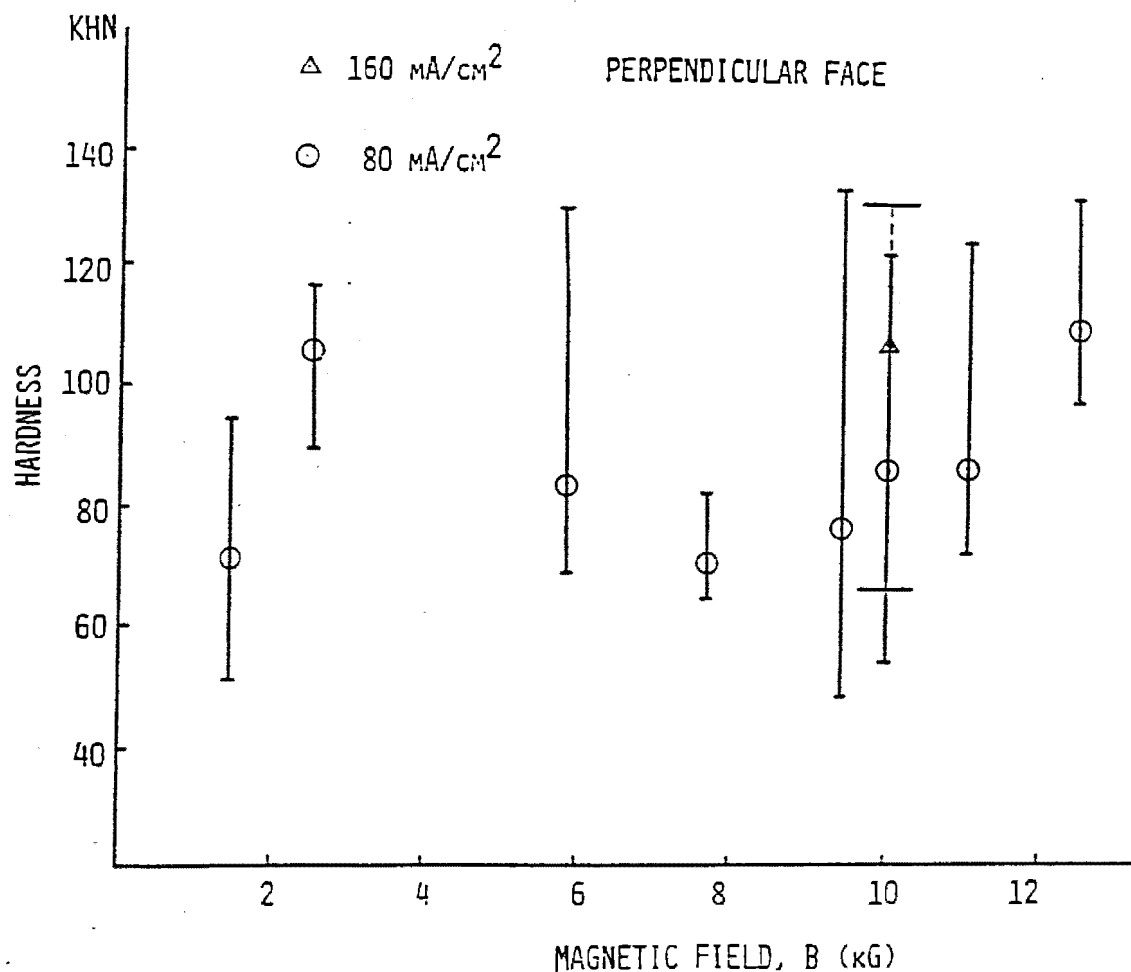


Figure 23. Effect of a magnetic field on microhardness. Hardness was measured on a cross section surface perpendicular to the magnetic field (see Fig. 6). The smaller cell without a water jacket was used. At 10 kG, one deposit made at 160 mA/cm² is shown.

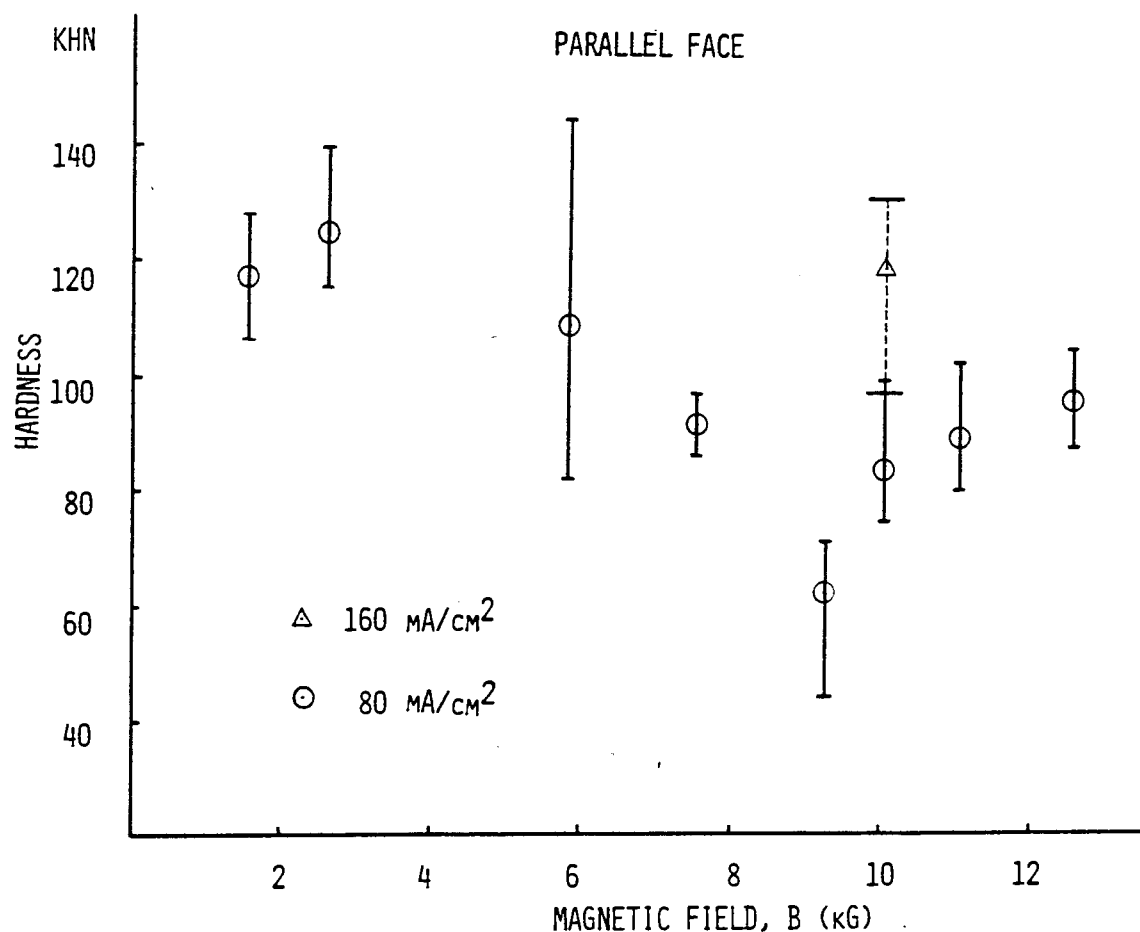


Figure 24. Effect of a magnetic field on microhardness. Hardness was measured on a cross section surface parallel to the magnetic field (see Fig. 6). The smaller diameter cell without water jacket was used. At 10 kG, one deposit made at 160 mA/cm² is shown.

TABLE V

HARDNESS OF DEPOSITS AND SUBSTRATE @ CD = 80.0 mA/sq cm
 WITH LARGER TEMPERATURE CONTROLLED CELL
 FIVE INDENTATIONS EACH, WITH A 50 GM LOAD

RUN #	B KG	ORIENT*	DEPOSIT KHN			SUBSTRATE KHN		
			AVG	LO	HI	AVG	LO	HI
111	OUT	$\frac{1}{11}$	INSUFF DEPOSIT			77	64	93
				"		64	60	70
110	0.074	$\frac{1}{11}$		"		72	65	83
				"		63	52	76
71	0.55	$\frac{1}{11}$		"		73	70	84
				"		61	49	65
72	0.95	$\frac{1}{11}$		"		62	55	69
				"		62	51	70
73	1.40	$\frac{1}{11}$	48	38	58	66	52	80
			60	50	67	67	53	89
103	1.40	$\frac{1}{11}$	59	49	65	57	50	61
			58	46	74	58	50	64
74	1.80	$\frac{1}{11}$	67	58	77	63	61	65
			67	56	73	58	50	64
75	2.20	$\frac{1}{11}$	63	55	73	49	41	52
			62	48	86	56	48	61
94	2.80	$\frac{1}{11}$	64	55	67	58	51	70
			66	51	87	55	51	60
96	3.20	$\frac{1}{11}$	80	66	94	55	49	60
			72	37	88	49	37	58
97	3.20	$\frac{1}{11}$	75	64	88	57	46	63
			63	46	73	49	37	58
95	3.60	$\frac{1}{11}$	87	83	100	59	50	71
			79	65	97	53	43	64
76	4.20	$\frac{1}{11}$	68	62	74	53	47	59
			63	54	73	57	50	65

TABLE V (CONTINUED)

70	4.20	$\frac{1}{11}$	88 115	62 100	114 131	50 66	43 61	60 80
98	4.80	$\frac{1}{11}$	91 108	79 105	106 117	65 62	59 54	72 70
99	5.50	$\frac{1}{11}$	96 102	77 94	118 109	58 69	44 64	70 72
100	6.00	$\frac{1}{11}$	89 81	76 73	97 88	62 63	58 57	73 62
101	6.50	$\frac{1}{11}$	81 89	58 70	100 109	54 72	36 59	68 86
102	6.90	$\frac{1}{11}$	73 77	62 64	78 86	58 70	53 62	71 76
77	7.40	$\frac{1}{11}$	124 109	120 83	131 124	62 67	52 63	70 71

*For definition of orientation see Figure 6 in Chptr. 2.

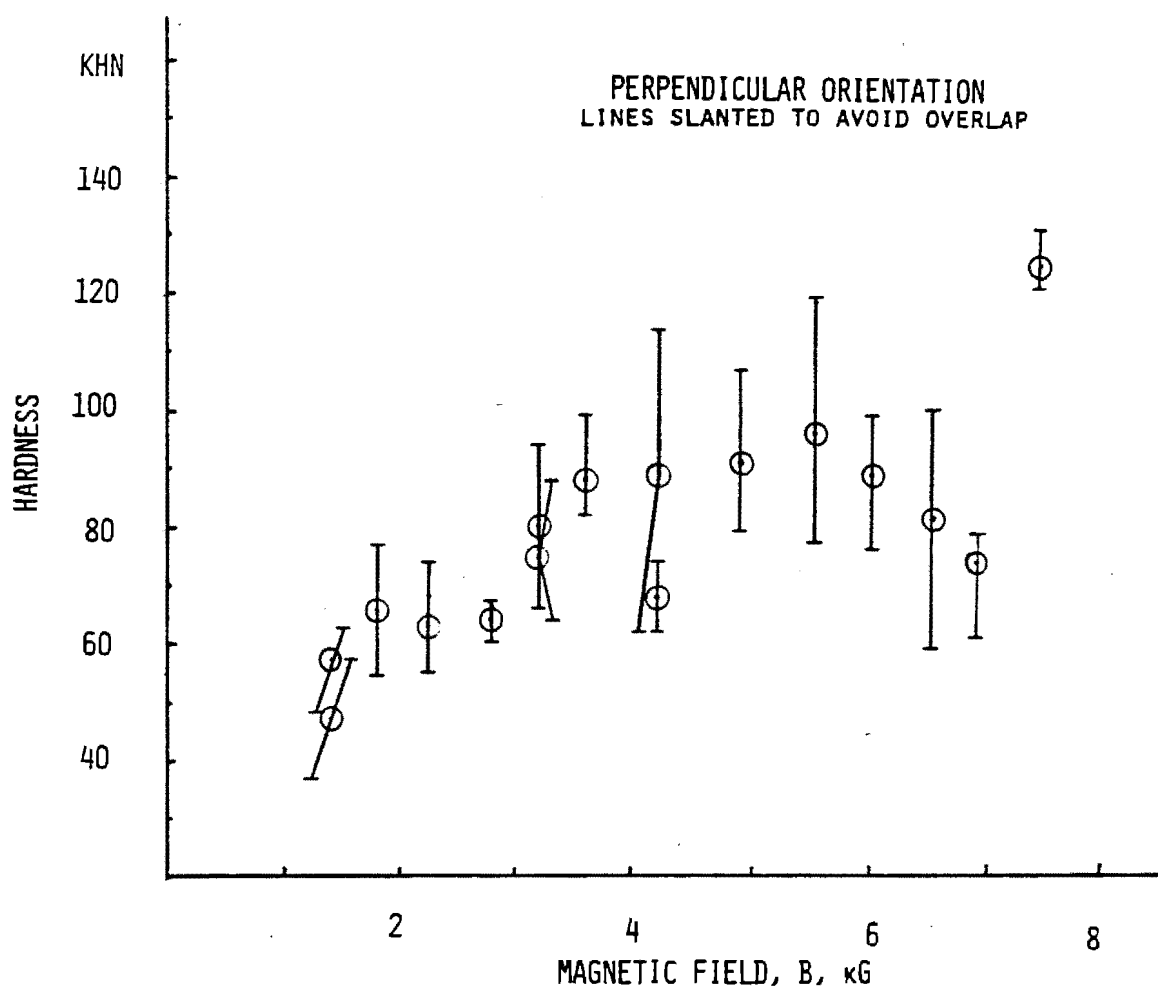


Figure 25. Effect of a magnetic field on microhardness. The data from Table 5 is plotted. Hardness was measured on a cross section surface perpendicular to the magnetic field (see Fig. 6). The larger diameter cell with a water jacket was used. The current density was 80 mA/cm².

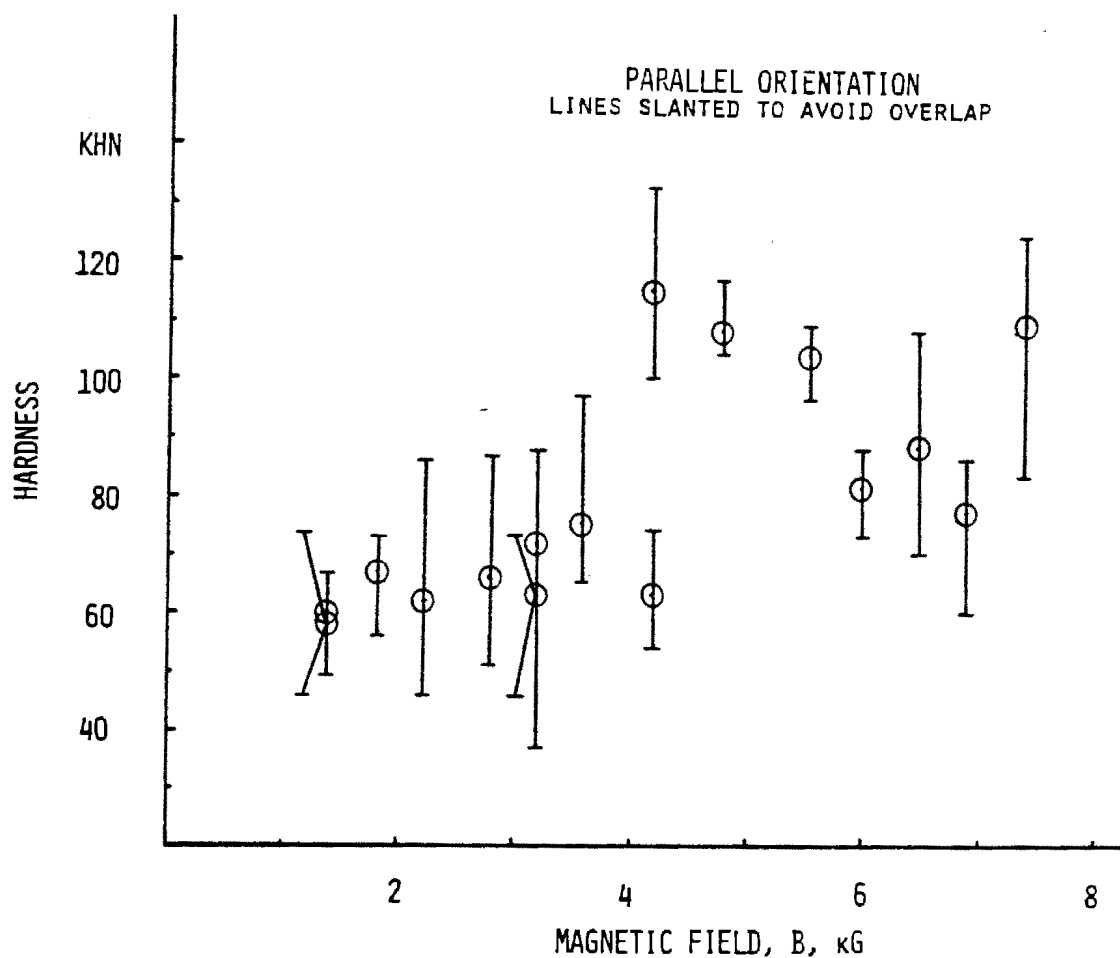


Figure 26. Effect of a magnetic field on microhardness. The data from Table 5 is plotted. Hardness was measured on a cross section surface parallel to the magnetic field (see Fig. 6). The larger diameter cell with a water jacket was used. The current density was 80 mA/cm² for all deposits shown.

clearly drawn.

In Figures 24 and 26 the deposits at 1.4 kG (runs 73, 103) and 3.2 kG (runs 96, 97) show fairly good hardness reproducibility, but the deposit at 4.2 kG (70, 76) shows poor reproducibility especially in the parallel orientation.

For the deposits at higher current density only those deposits at 190 through 320 mA/sq cm were compact and uniform enough to find the hardness. The results are shown in Table VI and Figure 27 for both the parallel and perpendicular orientation.

DISCUSSION

From their work, Valentine and Lamb (18) concluded that hardness has a low correlation to the other mechanical properties such as tensile strength, electrical resistivity and cathode polarization, and that "there is a vague parallel correlation between tensile strength and hardness." In comparison to measurements of the tensile strength some parallelism was found by these workers for deposits produced at 5 to 40 mA/sq cm. However, for deposits with similar tensile strengths poor correlation or opposite trends were found upon comparing hardness and tensile results. At the same time, they found that higher tensile strength deposits tend to be harder.

Although Lamb and Valentine (18) found that the

TABLE VI

HARDNESS OF DEPOSITS AND SUBSTRATE @ HIGH CURRENT DENSITY
 B = 7.40 KG W/TEMPERATURE CONTROLLED CELL
 FIVE INDENTATIONS EACH, WITH A 50 GM LOAD

RUN #	CD mA/sq cm	ORIENT*	DEPOSIT KHN			SUBSTRATE KHN		
			AVG	LO	HI	AVG	LO	HI
78	190	$\frac{1}{11}$	67	40	83	51	47	53
			64	51	82	48	47	69
80	190	$\frac{1}{11}$	67	38	98	53	52	65
			80	67	88	61	57	65
104	240	$\frac{1}{11}$	88	77	97	59	54	66
			87	80	99	64	61	72
81	250	$\frac{1}{11}$	87	69	107	60	43	76
			78	73	82	69	61	85
83	280	$\frac{1}{11}$	67	53	79	60	57	67
			78	63	85	60	52	65
113	320	$\frac{1}{11}$	98	74	124	57	53	62
			97	79	114	61	54	70

*For definition of orientation see Figure 6 in Chptr. 2.

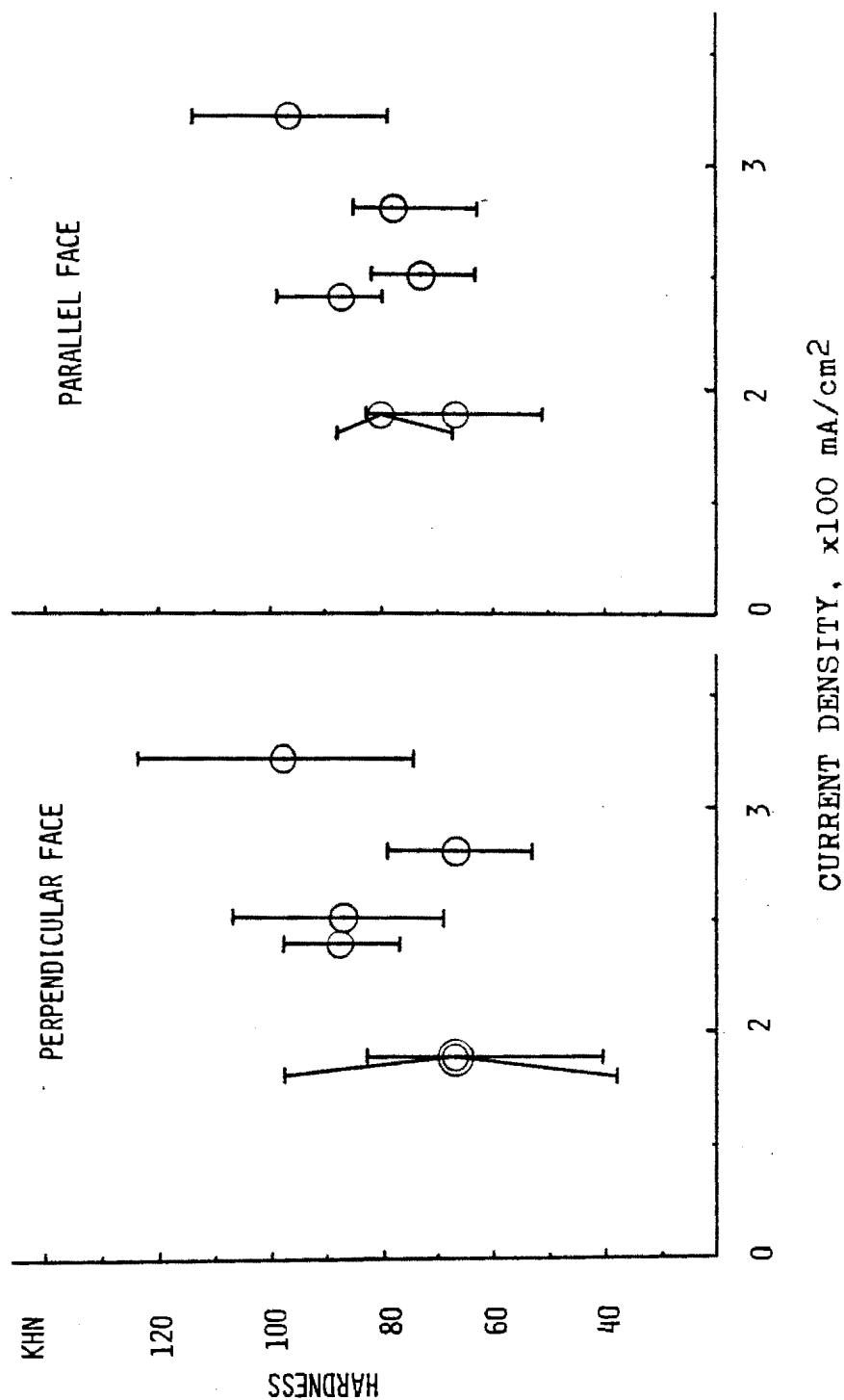


Figure 27. Effect of current density on microhardness. The data from Table 6 is plotted. Hardness measured on both perpendicular and parallel surfaces is shown (see Fig. 6). The larger diameter cell with a water jacket was used. The magnetic field for each experiment was 7.40 kG.

hardness for non-addition agent deposits were in the range from 45 to 60 KHN (200 gm load; with a 50 gm load about 11 KHN higher) and the range for most individual deposits was ± 5 KHN, our results show a maximum range of over ± 20 KHN for 5 indentations and a 50 gm load. Furthermore, their hardest specimen was 148 KHN with a gelatine additive. Without any additive, our highest average hardness was 124 KHN in run 77 at 7.4 kG and 80 mA/sq cm.

At very low current densities (5 to 20 mA/sq cm), Lamb and Valentine (18) report deposits where long columnar structures are seen which extend completely through the deposits. At lower current densities the structure of the substrate tends to be preserved because ions arriving at the surface of the electrode have sufficient time to surface diffuse to a stable edge or kink location before other ions arrive where they are incorporated into the existing structure. (15, p.48). At higher current densities, three dimensional nuclei are energetically favored since ions are arriving so quickly that the ions have no time to diffuse to sites which would preserve the previous layer of deposit (9, p.189, 15, p.9).

Vagramyan and Solov'eva (25) note the work of D.J. Macnaughton which states that hardness is related to the grain size of the deposit. The notion behind this is that the vast number of grain boundaries which exist in a

deposit with very small grains blocks the movement of dislocations which is necessary for plastic deformation to occur.

Surface-active and colloidal additives such as gelatin, mollases, or albumin were not included in our solutions, but these additives can be used to alter the grain structure as mentioned in the section on uniformity of the deposit. Furthermore, such additives alter not only mechanical but electrical properties as well since the additives are often codeposited (26).

Fedot'ev (26) found that an increase in the current density, decrease in temperature, increase in acidity, or decrease in the Cu(II) ion concentration will cause the production of finer-grained crystals. Also, he notes that the increase in polarization generally causes an increase in tensile strength and hardness. Such observations are related to the conclusions of Kortya, Dvorak and Bohagkova (27, p.300) which state that very small crystals have a high chemical free energy, and so for such crystals to be stable the concentration overpotential must be high.

Our data is as yet absent of any definitive, reproducible effect on hardness. However, these results are important in demonstrating the wide range of deposit characteristics which can be produced. The variety of the deposits produced is clearly shown in Figure 28. Presently, the usefulness of this information is somewhat

limited by the lack of predictability. Nonetheless, we feel capable of altering the characteristics of the deposit with only a manipulation of the current density and the application of a suitable magnetic field.

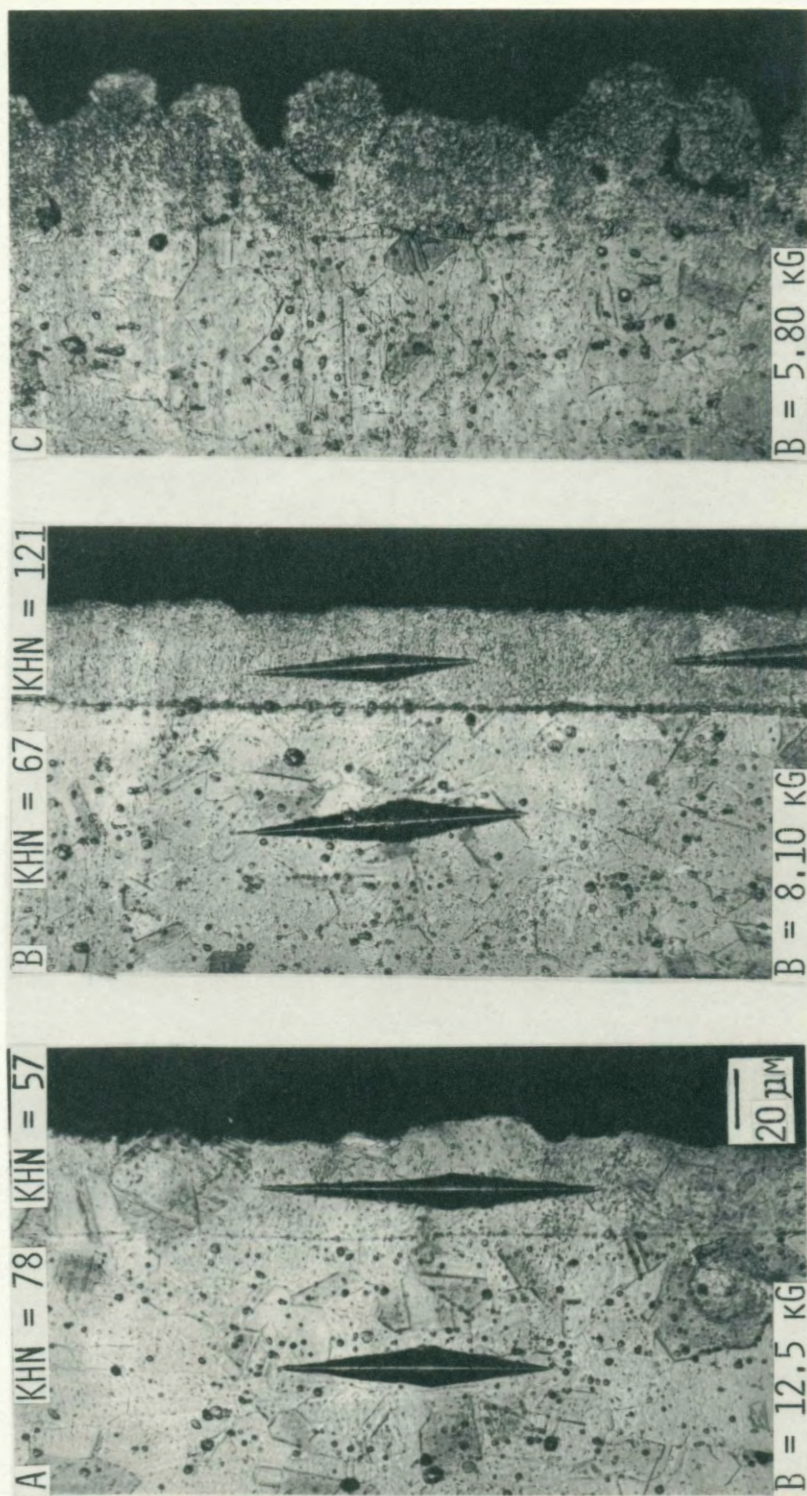


Figure 28. Variety of deposit characteristics obtained. The polished and etched cross section surfaces show Knoop hardness indentations made with a 50 gm load. Copper in A deposited at 180 mA/cm². Copper in B and C deposited at 160 mA/cm². Magnification marker shown in A applies to all photographs. C shows a deposit too rough to make hardness measurements.

CHAPTER VII

CONCLUSIONS

It appears quite clear from our results that the application of a magnetic field is effective in enhancing ion transport through the stirring effect produced by the magnetic force on charge carriers. Enhanced ion transport also aids in reducing the concentration overpotential which reduces the electrical potential that must be supplied for plating to occur. In addition the reduction of the concentration polarization allows the use of larger current densities without exceeding the limiting current. Lower average cell potential also means suppression of hydrogen production which causes a spongy deposit and low current efficiency.

The uniformity of the deposit can be altered by applying a suitable magnetic field, and this is also related to the magnetic force on charge carriers. The magnetoresistance, which arises from the deflection of ions due to the Lorentz force and also an ionic Hall-effect, are believed to be significant causes for the increased uniformity of the copper deposits. This improvement in uniformity is particularly visible in the deposits on the copper grids (Figure 14).

Our results also indicate that the application of a

magnetic field can affect the grain size of the deposits and the hardness without adding additives or altering the experimental conditions. In addition, deposits with a wide variety of deposit characteristics were obtained.

Further studies should be done with higher magnetic fields than were available in this work. The limiting current and properties of the deposits at these higher current densities and magnetic fields should be studied. Further work should be conducted on improvements in thinning uniformity.

REFERENCES

1. H. Takeo, S. Mai, and J. Dash, Proceedings of the 41st Annual Meeting of the Electron Microscopy Society of America , 274 (1983).
2. H. Takeo, C. Tam, and J. Dash, Proceedings of the AES 11th Symposium on Plating in the Electronics Industry , (1984).
3. J. Dash and K. Housen, Proceedings of the 38th Annual Meeting of the Electron Microscopy Society of America , 144 (1980).
4. A.R. Denaro, Elementary Electrochemistry , Butterworth's, London (1965).
5. Edmund C. Potter, Electrochemistry , Cleaver-Hume Press Ltd., London, (1961).
6. J.O'M. Bockris and A.K.N. Reddy, Modern Electrochemistry , Plenum Press, New York (1970).
7. Ernest H. Lyons, Jr., Introduction to Electrochemistry , D.C. Heath and Co., Boston (1967).
8. S. Mohanta and T.Z. Fahidy, Electrochim. Acta 19 , 835 (1974).
9. J.O'M. Bockris and D.M. Drazic, Electrochemical Science , Taylor and Francis, London (1972).
10. D. Laforgue-Kantzer, Electrochim. Acta 10 , 585 (1965).
11. P.L. Read and E. Katz, Physical Review Letters 5 , 466 (1960).
12. C. Cousins, M.S. Thesis, Portland State University, (1982).
13. S. Mohanta and T.Z. Fahidy, Electrochim. Acta 19 , 771 (1974).
14. J. Dash and M. Takeo, J. Appl. Phys. 55 , 2604 (1984).
15. E.H. Lyons, Jr., Modern Electroplating , Ed. F.A. Lowenheim, Wiley and Sons, Inc, New York, (1974).
16. J.W. Dini, Plating 51 , 119 (Feb. 1964).

17. S. Glasstone, Introduction to Electrochemistry ,
Van Nostrand Co., New York (1959).
18. Vernon A. Lamb and Donald R. Valentine, Plating 53 ,
86 (Jan. 1966).
19. D.G. Howard, Private Communication (1985).
20. J. Dash and W.W. King, J. Electrochem. Soc. 119(1) ,
51 (1972).
21. P. Csokan, Transactions of the Institute of Metal
Finishing 54 , 49 (1976).
22. H.V. Wildwood, M.S. Thesis, The University of
Waterloo, (1977).
23. W.J.McG. Tegart, The Electrolytic and Chemical
Polishing of Metals , Pergamon Press, London
(1959).
24. J. Dash, J. Roush, A. Trzynka, Unpublished Work (1985).
25. A.T. Vagramyan and Z.A. Solov'eva, Electroplating and
Metal Finishing 15 , 45 (1962).
26. N.P. Fedot'ev, Plating 53 , 309 (Mar. 1966).
27. J. Kortya, J. Dvorak and V. Bohagkova,
Electrochemistry , Methuen, London (1976).